JACS
ARTICLES

Synthesis, Structure, and Reactivity of 13-Vertex Carboranes and 14-Vertex Metallacarboranes

Liang Deng, Hoi-Shan Chan, and Zuowei Xie*

Contribution from the Department of Chemistry, The Chinese University of Hong Kong, Shatin, New Territories, Hong Kong, China

Received January 31, 2006; E-mail: zxie@cuhk.edu.hk

Abstract: Syntheses, properties, and synthetic applications of 13-vertex *closo*- and *nido*-carboranes are reported. Reactions of the *nido*-carborane salt $[(CH_2)_3C_2B_{10}H_{10}]Na_2$ with dihaloborane reagents afforded 13-vertex *closo*-carboranes 1,2-$(CH_2)_3$-3-R-1,2-$C_2B_{11}H_{10}$ (R = H (**2**), Ph (**3**), *Z*-EtCH=C(Et) (**4**), *E*-^{t}BuCH=CH (**5**)). Treatment of the *arachno*-carborane salt $[(CH_2)_3C_2B_{10}H_{10}]Li_4$ with $HBBr_2 \cdot SMe_2$ gave both the 13-vertex carborane **2** and a 14-vertex *closo*-carborane $(CH_2)_3C_2B_{12}H_{12}$ (**8**). On the other hand, the reaction of $[C_6H_4(CH_2)_2C_2B_{10}H_{10}]Li_4$ with $HBBr_2 \cdot SMe_2$ generated only a 13-vertex *closo*-carborane 1,2-$C_6H_4(CH_2)_2$-1,2-$C_2B_{11}H_{11}$ (**9**). Electrophilic substitution reactions of **2** with excess MeI, Br_2, or I_2 in the presence of a catalytic amount of $AlCl_3$ produced the hexa-substituted 13-vertex carboranes 8,9,10,11,12,13-X_6-1,2-$(CH_2)_3$-1,2-$C_2B_{11}H_5$ (X = Me (**10**), Br (**11**), I (**12**)). The halogenated products **11** and **12** displayed unexpected instability toward moisture. The 13-vertex *closo*-carboranes were readily reduced by groups 1 and 2 metals. Accordingly, several 13-vertex *nido*-carborane dianionic salts {*nido*-1,2-$(CH_2)_3$-1,2-$C_2B_{11}H_{11}$}{$Li_2(DME)_2(THF)_2$} (**13**), [{*nido*-1,2-$(CH_2)_3$-1,2-$C_2B_{11}H_{11}$}{$Na_2(THF)_4$}]$_n$ (**13a**), [{*nido*-1,2-$(CH_2)_3$-3-Ph-1,2-$C_2B_{11}H_{10}$}{$Na_2(THF)_4$}]$_n$ (**14**), [{*nido*-1,2-$C_6H_4(CH_2)_2$-1,2-$C_2B_{11}H_{11}$}{$Na_2(THF)_4$}]$_n$ (**15**), and {*nido*-1,2-$(CH_2)_3$-1,2-$C_2B_{11}H_{11}$}{$M(THF)_5$} (M = Mg (**16**), Ca (**17**)) were prepared in good yields. These carbon-atom-adjacent *nido*-carboranes were not further reduced to the corresponding *arachno* species by lithium metal. On the other hand, like other *nido*-carborane dianions, they were useful synthons for the production of supercarboranes and supra-icosahedral metallacarboranes. Interactions of **13a** with $HBBr_2 \cdot SMe_2$, (dppe)$NiCl_2$, and (dppen)$NiCl_2$ gave the 14-vertex carborane **8** and nickelacarboranes $[\eta^5\text{-}(CH_2)_3C_2B_{11}H_{11}]$Ni(dppe) (**18**) and $[\eta^5\text{-}(CH_2)_3C_2B_{11}H_{11}]$Ni(dppen) (**19**), respectively. All complexes were fully characterized by various spectroscopic techniques and elemental analyses. Some were further confirmed by single-crystal X-ray diffraction studies.

Introduction

Icosahedral carboranes constitute a class of structurally unique molecules with exceptional thermal and chemical stabilities and with the ability to hold various substituents.[1] These properties have made them useful basic units for weakly coordinating anions,[2] boron neutron capture therapy (BNCT) drugs,[3] and supramolecular design.[4] The chemistry of sub-icosahedral carboranes is also well developed.[1,5] In sharp contrast, supercarboranes with more than 12 vertices ($C_2B_nH_{n+2}$ with $n > 10$) were totally unknown until the first 13-vertex carborane 1,2-$C_6H_4(CH_2)_2$-3-Ph-1,2-$C_2B_{11}H_{10}$ was reported in 2003.[6] Subsequently, the first 14-vertex carborane 1,2-$(CH_2)_3$-1,2-$C_2B_{12}H_{12}$ was successfully synthesized in 2005.[7] The use of CAd (carbon-atom-adjacent) carborane anions as starting materials is the key to accomplishing such a breakthrough.[6−8]

---

(1) (a) Grimes, R. N. *Carboranes*; Academic Press: New York, 1970. (b) Onak, T. Polyhedral Carbaboranes. In *Comprehensive Organometallic Chemistry II*; Abel, E. W., Stone, F. G. A., Wilkinson, G., Eds. Pergamon: New York, 1995; Vol. 1, pp 217−255. (c) Grimes, R. N. Metallacarboranes. In *Comprehensive Organometallic Chemistry II*; Abel, E. W., Stone, F. G. A., Wilkinson, G., Eds.; Pergamon: New York, 1995; Vol. 1, pp 373−430. (d) Davidson, M.; Hughes, A. K.; Marder, T. B.; Wade, K. *Contemporary Boron Chemistry*; Royal Society of Chemistry: Cambridge, U.K., 2000. (e) Bubnov, Y. N. *Boron Chemistry at the Beginning of the 21st Century*; Russian Academy of Sciences: Moscow, Russia, 2002.

(2) For reviews, see: (a) Strauss, S. H. *Chem. Rev.* **1993**, *93*, 927−942. (b) Reed, C. A. *Acc. Chem. Res.* **1998**, *31*, 133−139. (c) Krossing, I.; Raabe, I. *Angew. Chem., Int. Ed.* **2004**, *43*, 2066−2090.

(3) For recent reviews, see: (a) Barth, R. F.; Soloway, A. H.; Fairchild, R. G. *Cancer Res.* **1990**, *50*, 1061−1070. (b) Yamamoto, Y. *Pure. Appl. Chem.* **1991**, *63*, 423−426. (c) Hawthorne, M. F. *Angew. Chem., Int. Ed. Engl.* **1993**, *32*, 950−984. (d) Hawthorne, M. F.; Maderna, A. *Chem. Rev.* **1999**, *99*, 3421−3434. (e) Valliant, J. F.; Guenther, K. J.; King, A. S.; Morel, P.; Schaffer, P.; Sogbein, O. O.; Stephenson, K. A. *Coord. Chem. Rev.* **2002**, *232*, 173−230.

(4) (a) Yang, X.; Jiang, W.; Knobler, C. B.; Hawthorne, M. F. *J. Am. Chem. Soc.* **1992**, *114*, 9719−9722. (b) Andrews, P. C.; Hardie, M. J.; Raston, C. L. *Coord. Chem. Rev.* **1999**, *189*, 169−198. (c) Schwab, P. F. H.; Levin, M. D.; Michl, J. *Chem. Rev.* **1999**, *99*, 1863−1934. (d) Wedge, T. J.; Hawthorne, M. F. *Coord. Chem. Rev.* **2003**, *240*, 111−128. (e) Vicente, J.; Chicote, M.-T.; Alvarez-Falcón, M. M. *Organometallics* **2003**, *22*, 4792−4797. (f) Jude, H.; Disteldorf, H.; Fischer, S.; Wedge, T.; Hawkridge, A. M.; Arif, A. M.; Hawthorne, M. F.; Muddiman, D. C.; Stang, P. J. *J. Am. Chem. Soc.* **2005**, *127*, 12131−12139. (g) Ma, L.; Hamdi, J.; Huang, J.; Hawthorne, M. F. *Inorg. Chem.* **2005**, *44*, 7249−7258. (h) Herzog, A.; Jalisatgi, S. S.; Knobler, C. B.; Wedge, T. J.; Hawthorne, M. F. *Chem.—Eur. J.* **2005**, *11*, 7155−7174.

(5) (a) Štíbr, B. *Chem. Rev.* **1992**, *92*, 225−250. (b) Siebert, W.; Maier, C.-J.; Maier, A.; Greiwe, P.; Bayer, M. J.; Hofmann, M.; Pritzkow, H. *Pure Appl. Chem.* **2003**, *75*, 1277−1286. (c) Grimes, R. N. *Pure Appl. Chem.* **2003**, *75*, 1211−1218. (d) Hosmane, N. S.; Maguire, J. A. *Organometallics* **2005**, *24*, 1356−1389.

(6) Burke, A.; Ellis, D.; Giles, B. T.; Hodson, B. E.; MacGregor, S. A.; Rosair, G. M.; Welch, A. J. *Angew. Chem., Int. Ed.* **2003**, *42*, 225−228.

(7) Deng, L.; Chan, H.-S.; Xie. Z. *Angew. Chem., Int. Ed.* **2005**, *44*, 2128−2131.

10.1021/ja0605772 CCC: $33.50 © 2006 American Chemical Society

These achievements open up possibilities for the development of new chemistry of super-carboranes and a new generation of BNCT drugs having a higher boron content.[9] This virtually unexplored area of research is especially attractive in view of the flourish chemistry displayed by their icosahedral cousins.[1−4,10] Herein, we would like to present our detailed study on the synthesis, structure, and reactivity of 13-vertex carboranes. Effects of the C, C′-linkages and RBX_2 reagents on the formation and reactivity of 13-vertex carboranes will be discussed, and the similarities and differences between the 12- and 13-vertex carboranes will also be addressed. Supra-icosahedral metallacarboranes derived from 13-vertex species will be described.

Results and Discussion

Synthesis and Structure of 13-Vertex *closo*-Carboranes. Our previous work showed that the linkages between the two cage carbon atoms of *o*-carboranes can control the relative positions of the cage carbon atoms during the reactions with group 1 metals.[8] Recent results indicated that these bridges may also play a role in stabilizing super-carboranes.[6,7] Considering the rigidity and relatively small size of the $(CH_2)_3$ unit, which may facilitate the capitation reaction with RBX_2, 1,2-$(CH_2)_3$-1,2-$C_2B_{10}H_{10}$ (**1**)[7] was chosen as the starting material. Reduction of **1** with excess finely cut sodium metal in THF at room temperature gave presumably a *nido*-carborane salt {1,2-$(CH_2)_3$-1,2-$C_2B_{10}H_{10}$}{$Na_2(THF)_x$}. Treatment of this salt with 2 equiv of dihaloborane reagents in toluene from −78 to 25 °C afforded, after column chromographic separation, 13-vertex carboranes 1,2-$(CH_2)_3$-3-R-1,2-$C_2B_{11}H_{10}$ (R = H (**2**), Ph (**3**), *Z*-EtCH=C(Et) (**4**), *E*-^{t}BuCH=CH (**5**)) in 20−37% isolated yields (Scheme 1). A small amount of **1** (3−6%) and a mixture of other boron-containing compounds were obtained in all cases. Many attempts to separate these boron-containing species failed. The control experiments indicated that the use of 2 equiv of dihaloborane reagents offered the highest isolated yield of 13-vertex carboranes. It was assumed that some boranes might be consumed by side reactions. More than 2 equiv of boranes were not necessary, which resulted in difficulty in separation. Donor solvents such as THF, DME, and Et_2O led to a much lower yield.

In view of the isolated yield of 20% for **3** versus 6% for 1,2-$C_6H_4(CH_2)_2$-3-Ph-1,2-$C_2B_{11}H_{10}$,[6] it was suggested that **1** was a much better starting material than 1,2-$C_6H_4(CH_2)_2$-1,2-$C_2B_{10}H_{10}$. Such differences could be ascribed to the presence of the more sterically demanding *o*-xylyl bridge. This assumption was supported by the following experiments. Reaction of the *arachno*-carborane salt [{1,2-$(CH_2)_3$-1,2-$C_2B_{10}H_{10}$}{$Li_4(THF)_5$}]$_2$ (**6**) with 5.0 equiv of $HBBr_2$•SMe_2 gave both the 13-vertex carborane 1,2-$(CH_2)_3$-1,2-$C_2B_{11}H_{11}$ (**2**) and a 14-vertex carborane 1,2-$(CH_2)_3$-1,2-$C_2B_{12}H_{12}$ (**8**) in 32% and 7% yields,[7] respectively. However, treatment of the *arachno*-carborane salt [{1,2-$C_6H_4(CH_2)_2$-1,2-$C_2B_{10}H_{10}$}{$Li_4(THF)_6$}]$_2$ (**7**)[8a] with 5.0 equiv of $HBBr_2$•SMe_2 afforded only a 13-vertex carborane 1,2-$C_6H_4(CH_2)_2$-1,2-$C_2B_{11}H_{11}$ (**9**), and no 14-vertex species was detected (Scheme 2). These results suggested that the linkage played an important role in the preparation of super-carboranes. Single-crystal structures of **6** and **7** may offer some insight into these differences. The *o*-xylyl moiety in **7** folds toward the C_2B_3 face,[8a] which may limit the access of the borane reagents to the open pentagonal bonding face. On the other hand, the trimethylene group has no interaction with the hexagonal C_2B_4 or pentagonal C_2B_3 face.[8d]

Scheme 1. Preparation of 13-Vertex Carboranes from *nido* Species

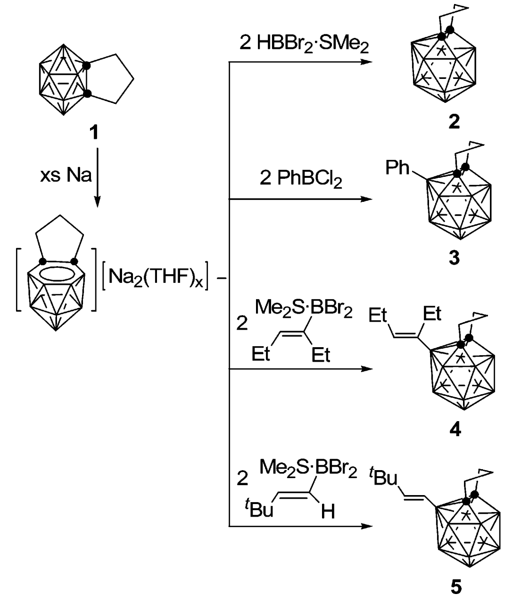

Scheme 2. Preparation of 13- and 14-Vertex Carboranes from *arachno* Species

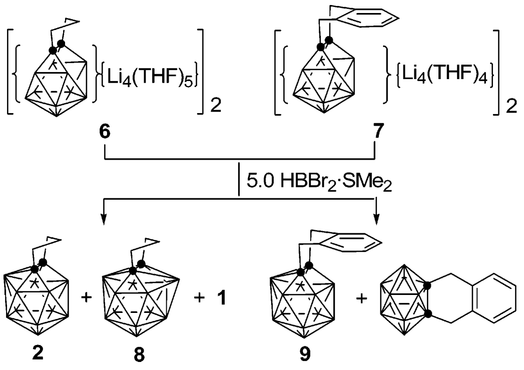

Compounds **2**−**5**, **8**, and **9** are quite stable in air and soluble in common organic solvents such as hexane, toluene, and THF. They were fully characterized by ^1H, ^{13}C, and ^{11}B NMR spectroscopic techniques as well as high-resolution mass spectrometry. Both the ^{11}B NMR spectra of **2** and **9** displayed a 1:5:5 splitting pattern, whereas those of **3**, **4**, and **5** showed the 1:1:3:2:4, 1:1:4:2:3, and 1:1:6:3 splitting patterns, respectively.

Single-crystal X-ray analyses revealed there are four and two crystallographically independent molecules, respectively, in the unit cells of **3** and **9**. Their representative structures are shown

---

[8] For CAd carborane anions, see: (a) Zi, G.; Li, H.-W.; Xie, Z. *Organometallics* **2001**, *20*, 3836−3838. (b) Zi, G.; Li, H.-W.; Xie, Z. *Chem. Commun.* **2001**, 1110−1111. (c) Zi, G.; Li, H.-W.; Xie, Z. *Organometallics* **2002**, *21*, 5415−5427. (d) Deng, L.; Cheung, M.-S.; Chan, H.-S.; Xie, Z. *Organometallics* **2005**, *24*, 6244−6249. (e) Xie, Z. *Pure Appl. Chem.* **2003**, *75*, 1335−1341.

[9] Grimes, R. N. *Angew. Chem., Int. Ed.* **2003**, *42*, 1198−1200.

[10] For reviews, see: (a) Saxena, A. K.; Hosmane, N. S. *Chem. Rev.* **1993**, *93*, 1081−1124. (b) Saxena, A. K.; Maguire, J. A.; Hosmane, N. S. *Chem. Rev.* **1997**, *97*, 2421−2462. (c) Grimes, R. N. *Coord. Chem. Rev.* **2000**, *200/202*, 773−811. (d) Xie, Z. *Pure Appl. Chem.* **2001**, *73*, 361−365. (e) Kang, S. O.; Ko, J. *Adv. Organomet. Chem.* **2001**, *47*, 61−99. (f) Xie, Z. *Acc. Chem. Res.* **2003**, *36*, 1−9. (g) Xie, Z. *Coord. Chem. Rev.* **2002**, *231*, 23−46. (h) Xie, Z. *Coord. Chem. Rev.* **2006**, *250*, 259−272.

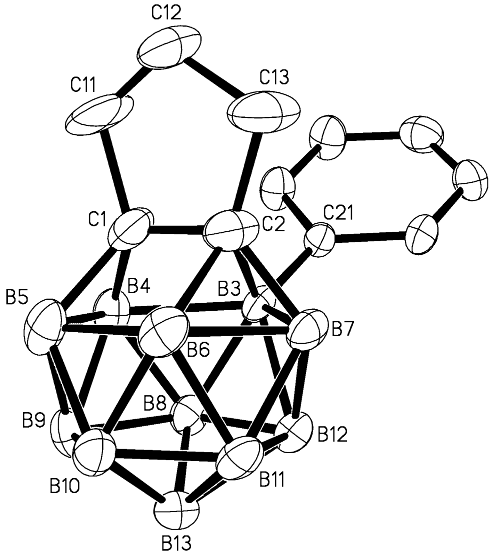

Figure 1. Molecular structure of 1,2-$(CH_2)_3$-3-Ph-1,2-$C_2B_{11}H_{10}$ (**3**), showing one of the four crystallographically independent molecules in the unit cell.

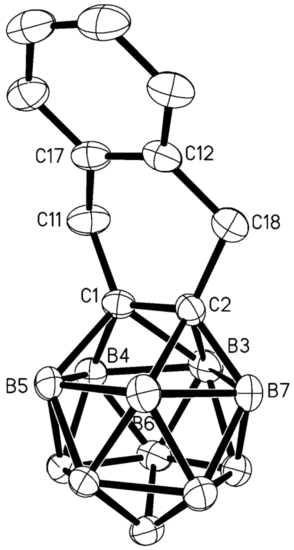

Figure 2. Molecular structure of 1,2-$C_6H_4(CH_2)_2$-1,2-$C_2B_{11}H_{11}$ (**9**), showing one of the two crystallographically independent molecules in the unit cell.

in Figures 1 and 2. Selected bond distances are listed in Table 1. In view of the molecular structures of **3**, **9**, and 1,2-C_6H_4-$(CH_2)_2$-3-Ph-1,2-$C_2B_{11}H_{10}$ (**9Ph**),[6] it is found that the connectivity of the cage carbon atoms in **3** is significantly different from those observed in **9** and **9Ph**. Chart 1 illustrates the connectivity of the C(cage)−C(cage) unit with its lower layered five boron atoms. The four independent molecules in **3** occur as two pairs of similar molecules, and each of them are related by an approximate translation. One pair (**3a**, **b**) bears two trapezoidal faces with the others being triangulated, giving one five- and one four-coordinate cage carbon atoms, respectively. The other (**3c**, **d**) possesses one trapezoidal face and one bent pentagonal face, resulting in the formation of two four-coordinate cage carbon atoms. It is noted that in solution only one set of peaks was observed in the ^{1}H and ^{11}B NMR spectra of **3**, indicating a fast diamond−square−diamond process.[11] Low-temperature NMR experiments were not able to arrest this transformation, implying a small activation barrier.[6] These results suggest that the tethering group has a large effect on the connectivity around the cage carbon atoms.

Methylation and Halogenation of 13-Vertex *closo*-Carboranes. Very rich electrophilic substitution reactions on icosahedral boranes[12] and carboranes[13,14] prompted us to examine the chemical properties of 13-vertex carboranes. Compound **2** was chosen for this purpose for its simplicity. Reaction of **2** with excess iodomethane in the presence of a catalytic amount of $AlCl_3$ at room temperature for 2 days gave a hexamethylated 13-vertex carborane 8,9,10,11,12,13-$(CH_3)_6$-1,2-$(CH_2)_3$-1,2-$C_2B_{11}H_5$ (**10**) in 85% isolated yield (Scheme 3). This reaction was closely monitored by ^{11}B NMR spectroscopy as **2** and **10** have distinct splitting patterns. Prolonged reaction did not lead to the complete methylation product but rather a mixture of polymethylated products as indicated by the ^{11}B NMR spectra. The hexahalogenated products 8,9,10,11,12,13-X_6-1,2-$(CH_2)_3$-1,2-$C_2B_{11}H_5$ (X = Br (**11**), I (**12**)) were obtained in 22% and 25% isolated yields by treatment of **2** with excess bromine and iodine in CH_2Cl_2 at room temperature in the presence of a catalytic amount of $AlCl_3$, respectively (Scheme 3). Higher halogenation products were not observed even under forced reaction conditions. Interaction of **2** with H_2O_2 led to a complete degradation of the cage, resulting in the formation of $B(OH)_3$, which differed significantly from its icosahedral analogues.[14h]

Compound **10** is very stable in air and moisture and quite soluble in common organic solvents. However, **11** and **12** are hygroscopic and decomposed slowly in moist air. Such a process sped up in a basic media as indicated by the ^{11}B NMR. These results are very different from those obtained for their icosahedral cousins,[12−14] which might be ascribed to the joint effects of the substituents and the more open trapezoidal faces presented in these 13-vertex carboranes. The low stability of **11** and **12**

---

(11) Lipscomb, W. *Science* **1966**, *153*, 373−378.

(12) For $B_{12}H_{12}^{2-}$, see: (a) Peymann, T.; Knobler, C. B.; Hawthorne, M. F. *J. Am. Chem. Soc.* **1999**, *121*, 5601−5602. (b) Peymann, T.; Knobler, C. B.; Khan, S. I.; Hawthorne, M. F. *Angew. Chem., Int. Ed.* **2001**, *40*, 1664−1667. (c) Peymann, T.; Knobler, C. B.; Khan, S. I.; Hawthorne, M. F. *J. Am. Chem. Soc.* **2001**, *123*, 2182−2185. (d) Sivaev, I. B.; Bregadze, V. I.; Sjoberg, S. *Collect. Czech. Chem. Commun.* **2002**, *67*, 679−727. (e) Farha, O. K.; Julius, R. L.; Lee, M. W.; Huertas, R. E.; Knobler, C. B.; Hawthorne, M. F. *J. Am. Chem. Soc.* **2005**, *127*, 18243−18251.

(13) For $CB_{11}H_{12}^{-}$, see: (a) Jelinek, T.; Plešek, J.; Heřmáneck, S.; Štíbr, B. *Collect. Czech. Chem. Commun.* **1986**, *51*, 819−829. (b) Jelinek, T.; Baldwin, P.; Scheidt, W. R.; Reed, C. A. *Inorg. Chem.* **1993**, *32*, 1982−1990. (c) Xie, Z.; Jelinek, T.; Bau, R.; Reed, C. A. *J. Am. Chem. Soc.* **1994**, *116*, 1907−1913. (d) King, B. T.; Janousek, Z.; Gruener, B.; Trammell, M.; Noll, B. C.; Michl, J. *J. Am. Chem. Soc.* **1996**, *118*, 3313−3314. (e) Xie, Z.; Manning, J.; Reed, R. W.; Mathur, R.; Boyd, P. D. W.; Benesi, A.; Reed, C. A. *J. Am.* Chem. Soc. **1996**, *118*, 2922−2928. (f) Xie, Z.; Tsang, C. W.; Xue, F.; Mak, T. C. W. *Inorg. Chem.* **1997**, *36*, 2246−2247. (g) Ivanov, S. V.; Rockwell, J. J.; Polyakov, O. G.; Gaudinski, C. M.; Anderson, O. P.; Solntsev, K. A.; Strauss, S. H. *J. Am. Chem. Soc.* **1998**, *120*, 4224−4225. (h) Xie, Z.; Tsang, C. W.; Sze, E. T. P.; Yang. Q.; Chan, D. T. W.; Mak, T. C. W. *Inorg. Chem.* **1998**, *37*, 6444−6451. (i) Tsang, C. W.; Xie, Z. *Chem. Commun.* **2000**, 1839−1840. (j) Clarke, A. J.; Ingleson, M. J.; Kociok-Köhn, G.; Mahon, M. F.; Patmore, N. J.; Rourke, J. P.; Ruggiero, G. D.; Weller, A. S. *J. Am. Chem. Soc.* **2004**, *126*, 1503−1517.

(14) For $C_2B_{10}H_{12}$, see: (a) Potenza, J. A.; Lipscomb, W. N. *Inorg. Chem.* **1966**, *5*, 1483−1488. (b) Bregadze, V. I. *Chem. Rev.* **1992**, *92*, 209−224. (c) Jiang, W.; Knobler, C. B.; Mortimer, M. D.; Hawthorne, M. F. *Angew. Chem., Int. Ed. Engl.* **1995**, *34*, 1332−1334. (d) Jiang, W.; Knobler, C. B.; Hawthorne, M. F. *Angew. Chem., Int. Ed.* **1996**, *35*, 2536−2537. (e) Herzog, A.; Knobler, C. B.; Hawthorne, M. F. *Angew. Chem., Int. Ed.* **1998**, *37*, 1552−1556. (f) Herzog, A.; Maderna, A.; Harakas, G. N.; Knobler, C. B.; Hawthorne, M. F. *Chem.*−*Eur. J.* **1999**, *5*, 1212−1217. (g) Herzog, A.; Callahan, R. P.; Macdonald, C. L. B.; Lynch, V. M.; Hawthorne, M. F.; Lagow, R. J. *Angew. Chem., Int. Ed.* **2001**, *40*, 2121−2123. (h) Herzog, A.; Knobler, C. B.; Hawthorne, M. F. *J. Am. Chem. Soc.* **2001**, *123*, 12791−12797. (i) Barberà, G.; Teixidor, F.; Viñas, C.; Sillanpää, R.; Kivekäs, R. *Eur. J. Inorg. Chem.* **2003**, *8*, 1511−1513. (j) Teixidor, F.; Barberà, G.; Vaca, A.; Kivekäs, R.; Sillanpää, R.; Oliva, J.; Viñas, C. *J. Am. Chem. Soc.* **2005**, *127*, 10158−10159.

Table 1. Selected Bond Distances (Å) in 13-Vertex Carboranes

	3a	3b	3c	3d	9a	9b	9Ph[a]	10	11
C(1)−B(3)	2.139(3)	2.109(3)	1.994(3)	2.102(3)	1.915(2)	1.907(2)	1.840(3)	2.167(9)	2.11(2)
C(1)−B(4)	1.635(3)	1.631(3)	1.567(3)	1.596(3)	1.622(2)	1.615(2)	1.569(3)	1.627(7)	1.60(2)
C(1)−B(5)	1.663(3)	1.687(3)	1.764(3)	1.681(3)	1.799(2)	1.799(2)	1.898(3)	1.627(7)	1.67(2)
C(1)−B(6)	2.173(3)	2.139(3)	2.382(3)	2.264(3)	2.404(2)	2.440(2)	2.373(3)	2.167(9)	2.24(2)
C(2)−B(3)	1.958(3)	1.877(2)	1.993(3)	1.978(3)	1.870(2)	1.867(2)	1.917(3)	1.860(9)	1.85(3)
C(2)−B(5)	2.588(3)	2.629(3)	2.470(3)	2.513(3)	2.526(2)	2.498(2)	2.587(3)	2.604(9)	2.56(2)
C(2)−B(6)	1.779(3)	1.803(3)	1.748(3)	1.774(3)	1.821(2)	1.820(2)	1.766(2)	1.860(9)	1.86(3)
C(2)−B(7)	1.539(3)	1.518(3)	1.539(3)	1.528(3)	1.591(2)	1.592(2)	1.632(3)	1.465(7)	1.53(2)
av B−X[b]								1.587(9)	1.94(1)

[a] See ref 6. [b] For **10**, X = Me; for **11**, X = Br.

Chart 1. Connectivity of the C(cage)−C(cage) Unit with Boron Atoms in 13-Vertex Carboranes[a]

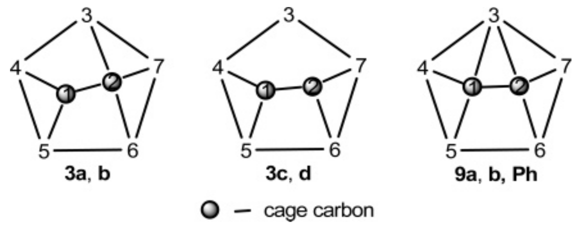

[a] The distance of 1.96 Å was arbitrarily chosen as the cutoff point for the representation of connectivities between the cage carbon and boron atoms.

Scheme 3. Methylation/Halogenation of 13-Vertex Carborane

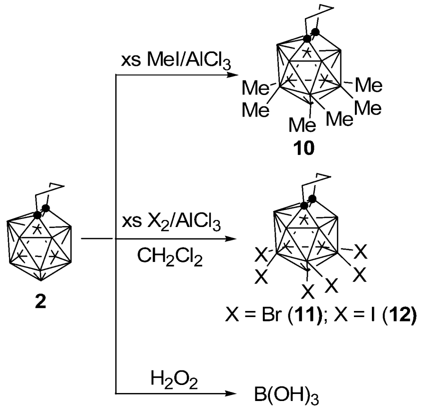

toward water especially basic solutions led to poor isolated yields, although they were formed quantitatively in the reactions according to the ^{11}B NMR analyses since the basic solutions were used to remove excess halogen reagents during the workup process.

The electronic effects of the substituents on the cage are significant as shown in Figure 3. According to the ^{11}B NMR chemical shifts of the B−Me, B−Br, and B−I vertices, it might be best described that both Me and Br are more electron-withdrawing[14j] and I is more electron-donating than the H atom in the 13-vertex cages. A similar phenomenon was observed in a 7,8,9,10,11,12-X_6−$CB_{11}H_6^-$ system.[13e]

The molecular structures of both **10** and **11** were further confirmed by single-crystal X-ray analyses and shown in Figures 4 and 5, respectively. The geometry of the cage and the connectivity around the cage carbon atoms in **10** and **11** are very similar to those of **3b** (Table 1). All six methyl or bromo substituents are bound to the cage boron atoms that are the farthest away from the cage carbons because these boron vertices are the most electron-rich ones. The average B−X bond distances of 1.587(9) Å in **10** and 1.94(1) Å in **11** are very close to those of 1.58 (1) Å in 4,5,7,8,9,10,11,12-$(CH_3)_8$-1,2-$C_2B_{10}H_4$,[14b] 1.60 (1) Å in 9-X-12-Y-3,4,5,6,7,8,9,10-$(CH_3)_8$-1,2-$C_2B_{10}H_4$ (X, Y = Cl, I),[14j] and 1.95 (1) Å in 9,10,11,12-Br_4-1,2-$(CH_3)_2$-1,2-$C_2B_{10}H_6$.[14a]

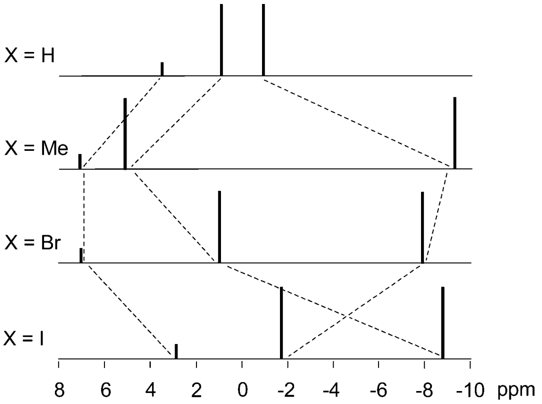

Figure 3. Stick representation of the chemical shifts and relative intensities in the $^{11}B\{^1H\}$ spectra of 1,2-$(CH_3)_2$-1,2-$C_2B_{11}H_5X_6$. The blue and black lines represent the BH and BX vertices, respectively.

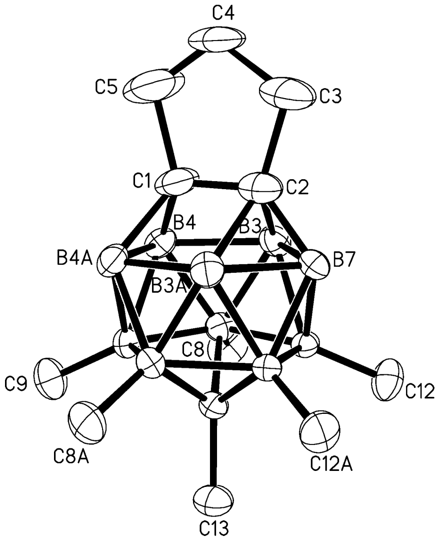

Figure 4. Molecular structure of 8,9,10,11,12,13-$(CH_3)_6$-1,2-$(CH_2)_3$-1,2-$C_2B_{11}H_5$ (**10**).

Reactions of 13-Vertex *closo*-Carboranes with Groups 1 and 2 Metals. Synthesis and Structure of 13-Vertex *nido*-Carborane Salts. It is well documented that *o*-$R_2C_2B_{10}H_{10}$ can be reduced by group 1 metals to form [*nido*-$R_2C_2B_{10}H_{10}$]M_2 or [*arachno*-$R_2C_2B_{10}H_{10}$]Li_4 (R_2 = linkages) salts.[8,15] They are very useful synthons for the synthesis of metallacarboranes of p-, d-, and f-block elements and super-carboranes with 13 and 14 vertices.[6,7,10,16] Treatment of 13-vertex *closo*-carboranes **2**, **3**,

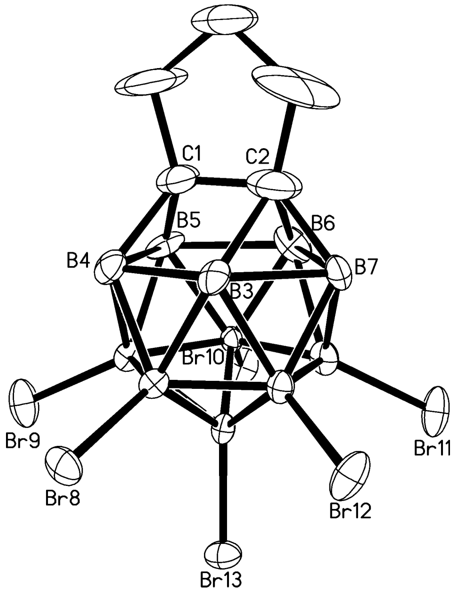

Figure 5. Molecular structure of 8,9,10,11,12,13-Br_6-1,2-$(CH_2)_3$-1,2-$C_2B_{11}H_5$ (**11**).

Scheme 4. Preparation of Group 1 Metal Complexes of 13-Vertex *nido*-Carboranes

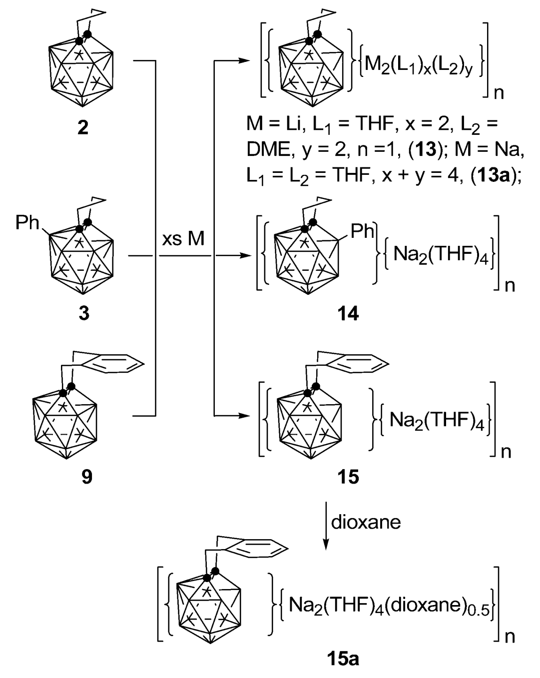

and **9** with excess finely cut Na metal in THF at room temperature gave the corresponding 13-vertex *nido*-carborane salts $[\{$*nido*-1,2-$(CH_2)_3$-1,2-$C_2B_{11}H_{11}\}\{Na_2(THF)_4\}]_n$ (**13a**), $[\{$*nido*-1,2-$(CH_2)_3$-3-Ph-1,2-$C_2B_{11}H_{10}\}\{Na_2(THF)_4\}]_n$ (**14**), and $[\{$*nido*-1,2-$(C_6H_4)(CH_2)_2$-1,2-$C_2B_{11}H_{11}\}\{Na_2(THF)_4\}]_n$ (**15**) in 80−85% yields (Scheme 4). It was noteworthy that these reactions proceeded much faster than those of icosahedral cages and naphthalene was not required, indicating that 13-vertex carboranes were more reactive than the 12-vertex ones.[8,15] Recrystallization of **15** from a dioxane solution afforded a *nido*-carborane salt of dioxane solvation $[\{$*nido*-1,2-$C_6H_4(CH_2)_2$-1,2-$C_2B_{11}H_{11}\}\{Na_2(dioxane)_{0.5}(THF)_4\}]_n$ (**15a**).

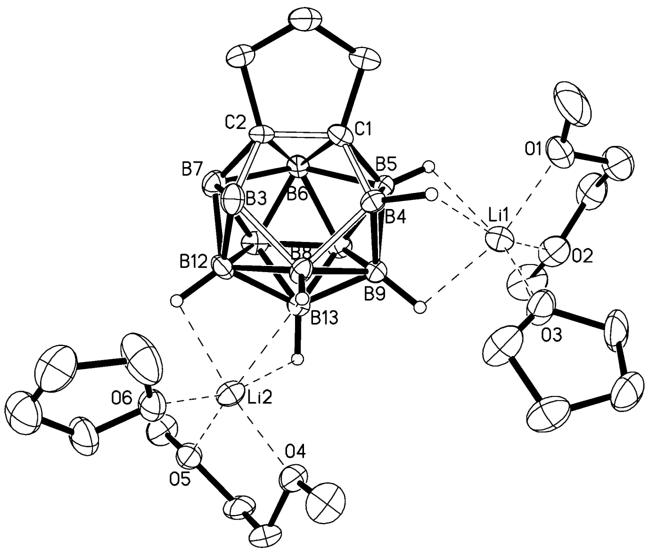

Figure 6. Molecular structure of $\{1,2\text{-}(CH_2)_3\text{-}1,2\text{-}C_2B_{11}H_{11}\}\{Li_2(DME)_2\text{-}(THF)_2\}$ (**13**).

Significantly different from **1**, the reaction of **2** with excess finely cut lithium metal in THF gave, after recrystallization from DME, $\{$*nido*-1,2-$(CH_2)_3$-1,2-$C_2B_{11}H_{11}\}\{Li_2(THF)_2(DME)_2\}$ (**13**) in 83% isolated yield. No *arachno* species was detected. This result indicates that the Li metal is unable to reduce the 13-vertex *nido*-carborane although Li can readily reduce the 12-vertex *nido*-carborane to the corresponding *arachno*-species.[8] It may be concluded that the 13-vertex *nido*-carborane is a stronger reductant (or a weaker oxidant) than the 12-vertex *nido*-carborane in the above redox reactions. This may be one of the reasons why 14-vertex carboranes are less accessible than the 13-vertex species.

The ^1H NMR spectra supported a ratio of two THF and two DME molecules per cage in **13**, four THF molecules per cage in **13a**, **14**, and **15** and four THF and a half dioxane molecules per cage in **15a**, respectively. The ^{11}B NMR spectra displayed a 1:5:5 splitting pattern in the range −9 to −25 ppm for **13**, **13a**, **15**, and **15a** and a 1:1:2:3:2:1:1 splitting pattern within −5 to −28 ppm for **14**. Their compositions were confirmed by elemental analyses. The molecular structures were subject to single-crystal X-ray diffraction studies.

Except for the monomeric structure of **13** that consists of well-separated, alternating layers of cations $[Li(THF)(DME)]^+$ and dianions $[$*nido*-$(CH_2)_3C_2B_{11}H_{11}]^{2-}$ shown in Figure 6, others are coordination polymers in which sodium ions link the *nido*-carborane cages via either Na···H−B interactions in **14** (Figure 7) and **15** (Figure 8) or Na···O(dioxane) bonding interactions

---

(15) For examples, see: (a) Dunks, G. B.; Wiersema, R. J.; Hawthorne, M. F. *J. Am. Chem. Soc.* **1973**, *95*, 3174−3179. (b) Tolpin, E. I.; Lipscomb, W. N. *Inorg. Chem.* **1973**, *12*, 2257−2262. (c) Churchill, M. R.; DeBoer, B. G. *Inorg. Chem.* **1973**, *12*, 2674−2682. (d) Getman, T. D.; Knobler, C. B.; Hawthorne, M. F. *J. Am. Chem. Soc.* **1990**, *112*, 4593−4594. (e) Chui, K.; Li, H.-W.; Xie, Z. *Organometallics* **2000**, *19*, 5447−5453.

(16) (a) Wilson, N. M. M.; Ellis, D.; Buoyd, A. S. F.; Giles, B. T.; Macgregor, S. A.; Rosair, G. M.; Welch, A. J. *Chem. Commun.* **2002**, 464−465. (b) Wang, S.; Wang, Y.; Cheung, M.-S.; Chan, H.-S.; Xie, Z. *Tetrahedron* **2003**, *59*, 10373−10380. (c) Laguna, M. A.; Ellis, D.; Rosair, G. M.; Welch, A. J. *Inorg. Chim. Acta* **2003**, *347*, 161−167. (d) Wang, S.; Li, H.-W.; Xie, Z. *Organometallics* **2004**, *23*, 3780−3787. (e) Wang, S.; Li, H.-W.; Xie, Z. *Organometallics* **2004**, *23*, 2469−2478. (f) Cheung, M.-S.; Chan, H.-S.; Xie, Z. *Organometallics* **2004**, *23*, 517−526. (g) Hodson, B. E.; McGrath, T. D.; Stone, F. G. A. *Organometallics* **2005**, *24*, 1638−1646. (h) Burke, A.; Ellis, D.; Ferrer, D.; Ormsby, D. L.; Rosair, G. M.; Welch, A. J. *Dalton Trans.* **2005**, 1716−1721. (i) Cheung, M.-S.; Chan, H.-S.; Xie, Z. *Organometallics* **2005**, *24*, 4468−4474. (j) Cheung, M.-S.; Chan, H.-S.; Bi, S.; Lin, Z.; Xie, Z. *Organometallics* **2005**, *24*, 4333−4336.

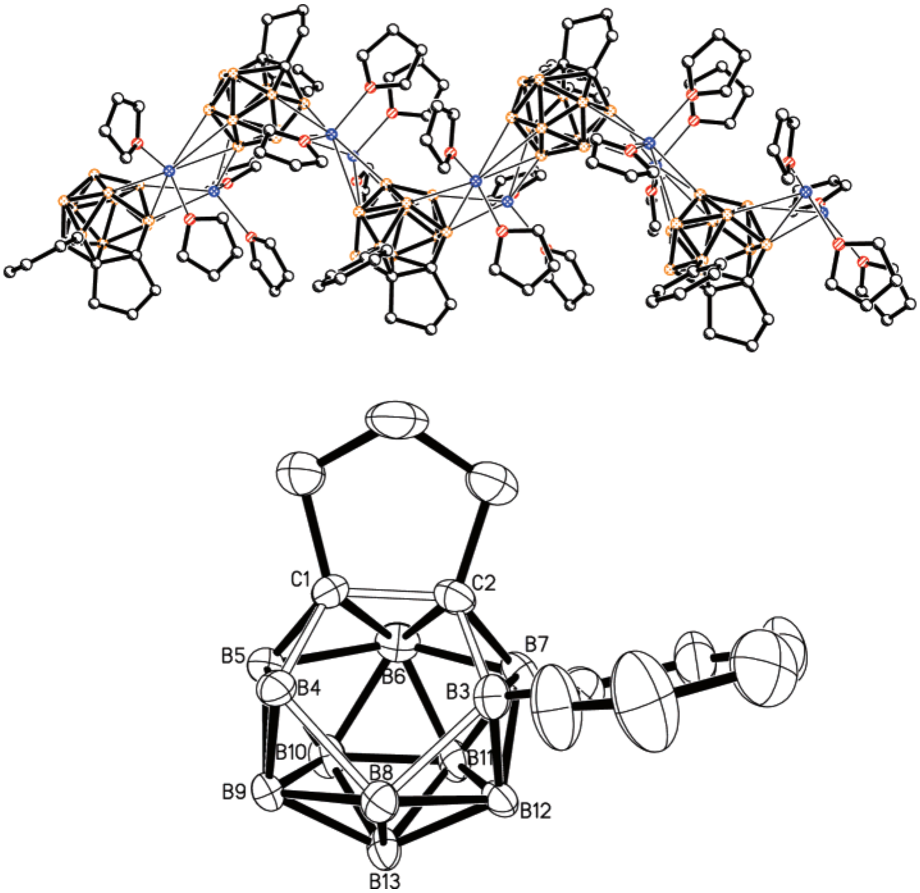

Figure 7. (Top) A portion of the infinite polymeric chains in $[\{1,2\text{-}(CH_2)_3\text{-}3\text{-}Ph\text{-}1,2\text{-}C_2B_{11}H_{10}\}\{Na_2(THF)_4\}]_n$ (**14**). (Bottom) Structure of the anion in **14**.

in **15a** (Figure 9) to form infinite zigzag polymeric chains. A common 13-vertex *nido*-carborane structural motif bearing an open five-membered face (C(1)C(2)B(3)B(4)B(8)) with a B(3)···B(4) separation of about 2.64 Å is observed in all structures. Selected bond distances are compiled in Table 2 for comparison. The out-of-plane (C(1)C(2)B(3)B(4)) displacement of the B(8) atom ranges from 0.68 to 0.72 Å, which is larger than those observed in 12-vertex *arachno*-carborane tetraanions (0.60 to 0.63 Å).[8d] The data in Table 2 indicate that the C, C′-linkages do not have significant effects on the geometry of the open five-membered ring in 13-vertex *nido*-carboranes.

To the best of our knowledge, there is no report on the reduction of boron-substituted *o*-carboranes.[17] Although it is not possible to determine which bond breaks first in the reduction of 13-vertex carboranes since complexes **13**−**15** are all thermodynamic products as indicated by the ^{11}B NMR spectroscopy (i.e., they do not isomerize upon heating), the formation of **14** suggests that the electron-withdrawing phenyl group favors the BPh vertex to be on the open five-membered face. Careful examination of the cage structures of **3** and **14** can conclude that this transformation clearly involves several bond-forming and bond-breaking processes.

It is reported that carboranes can be reduced by group 2 metals to form metallacarboranes.[18] As a more reactive species, 13-vertex *closo*-carboranes are readily reduced by alkaline earth metals. Treatment of **2** with excess activated Mg or Ca metal powder in THF at room temperature gave the alkaline earth metal complexes $\{(CH_2)_3C_2B_{11}H_{11}\}\{M(THF)_5\}$ (M = Mg (**16**), Ca (**17**)) in ~70% yield (Scheme 5). Their ^{11}B NMR spectra were identical with that of **13** and **13a**, indicating that they should have the same *nido*-carborane dianion. The ^{1}H NMR spectra supported a ratio of five THF molecules per cage for both **16** and **17**.

An X-ray diffraction study revealed that **17** is a monomeric structure, consisting of a 13-vertex $[nido\text{-}(CH_2)_3C_2B_{11}H_{11}]^{2-}$ dianion and a *pseudo*-octahedral complex cation as shown in Figure 10. The Ca^{2+} ion does not bond to the bent pentagonal face but rather interacts with the anion via one set of two Ca···H−B bondings. This is different from that of $[\eta^6\text{-}C_2B_{10}H_{12}]\text{-}Ca(MeCN)_4$ in which the *nido*-carboranyl ligand is η^6-bound to the Ca atom.[18a] As shown in Table 2, the structural parameters of the anions are very close to those observed in **13**.

Synthesis and Structure of 14-Vertex Metallacarboranes. Polyhedral expansion, a method originated by Hawthorne,[19] has been widely used in the preparation of supra-icosahedral metallacarboranes.[10,16,18,20] This prompted us to explore the

---

(17) The reduction of boron-substituted 12-vertex *nido*-carboranes $(Me_3Si)_4C_4B_7H_7(BMe)$ and $(Me_3Si)_4C_4B_7H_7(BSiMe_3)$ with Mg was reported, see: ref 18d.

(18) (a) Khattar, R.; Knobler, C. B.; Hawthorne, M. F. *J. Am. Chem. Soc.* **1990**, *112*, 4962−4963. (b) Khattar, R.; Knobler, C. B.; Hawthorne, M. F. *Inorg. Chem.* **1990**, *29*, 2191−2192. (c) Hosmane, N. S. *J. Organomet. Chem.* **1999**, *581*, 13−27. (d) Hosmane, N. S.; Zhang, H.; Maguire, J. A.; Wang, Y.; Demissie, T.; Colacot, T. J.; Ezhova, M. B.; Lu, K.-J.; Zhu, D.; Gray, T. G.; Helfert, S. C.; Hosmane, S. N.; Collins, J. D.; Baumann, F.; Kaim, W.; Lipscomb, W. N. *Organometallics* **2000**, *19*, 497−508. (e) Viñas, C.; Barberà, G.; Teixidor, F. *J. Organomet. Chem.* **2002**, *642*, 16−19. (f) Laromaine, A.; Teixidor, F.; Viñas, C. *Angew. Chem., Int. Ed.* **2005**, *44*, 2220−2222.

(19) Dunks, G. B.; McKown, M. M.; Hawthorne, M. F. *J. Am. Chem. Soc.* **1971**, *93*, 2541−2543.

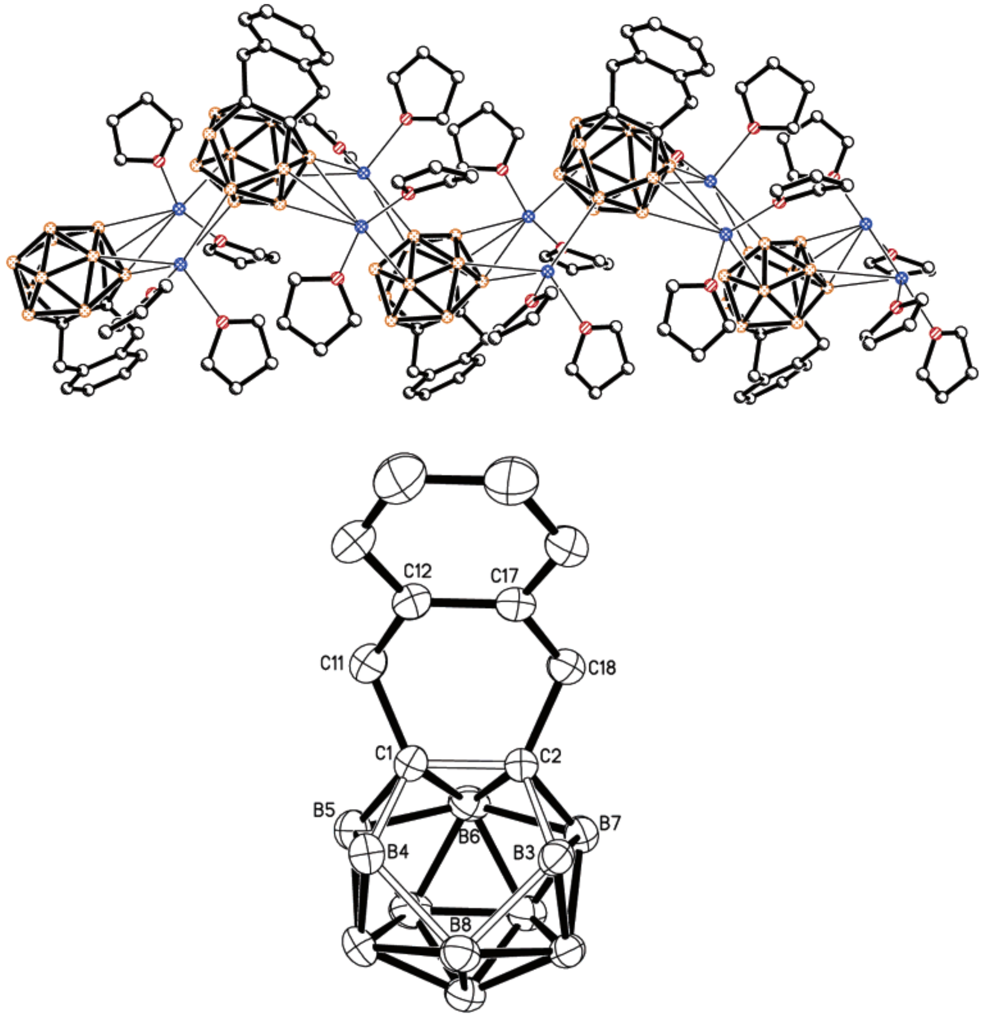

Figure 8. (Top) A portion of the infinite polymeric chains in $[\{1,2\text{-}C_6H_4(CH_2)_2\text{-}1,2\text{-}C_2B_{11}H_{11}\}\{Na_2(THF)_4\}]_n$ (**15**). (Bottom) Structure of the anion in **15**.

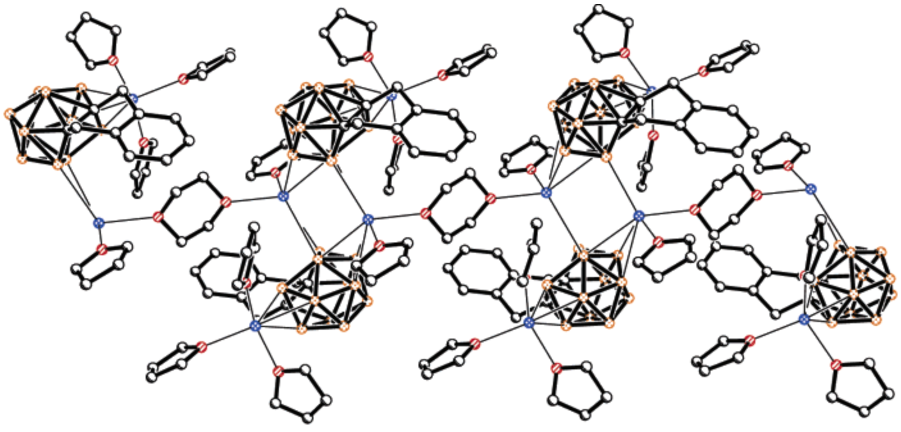

Figure 9. A portion of the infinite polymeric chains in $[\{1,2\text{-}C_6H_4(CH_2)_2\text{-}1,2\text{-}C_2B_{11}H_{11}\}\{Na_2(dioxane)_{0.5}(THF)_4\}]_n$ (**15a**).

applications of 13-vertex *nido*-carborane salts in the preparation of 14-vertex carboranes and metallacarboranes. Very recently we reported our preliminary results on the synthesis of a 14-vertex carborane $1,2\text{-}(CH_2)_3\text{-}1,2\text{-}C_2B_{12}H_{12}$ from the reaction of **13a** with $HBBr_2{\cdot}SMe_2$ in toluene.[7] Accordingly, we examined a series of reactions of **13a** with different kinds of metal salts such as $SnCl_2$, $ZrCl_4$, $(Ph_3P)_2NiCl_2$, $(Ph_3P)_2PdCl_2$, $(Ph_3P)_2PtCl_2$, and $(Ph_3P)_3RuCl_2$ in attempts to prepare 14-vertex metallacarboranes. The results showed that the neutral 13-vertex carborane **2** was generated quantitatively according to the ^{11}B NMR analyses and was recovered in more than 90% yield after workup in the reactions with $SnCl_2$, $ZrCl_4$, $(Ph_3P)_2PdCl_2$, and $(Ph_3P)_2PtCl_2$. It was clear that the redox reactions proceeded because

---

(20) For $M_2C_4B_8$ clusters, see: (a) Maxwell, W. M.; Bryan, R. F.; Sinn, E.; Grimes, R. N. *J. Am. Chem. Soc.* **1977**, *99*, 4016−4029. (b) Pipal, J. R.; Grimes, R. N. *Inorg. Chem.* **1978**, *17*, 6−10. (c) Maxwell, W. M.; Bryan, R. F.; Sinn, E.; Grimes, R. N. *J. Am. Chem. Soc.* **1977**, *99*, 4008−4015. For $M_2C_2B_{10}$ clusters, see: (d) Ellis, D.; Lopez, M. E.; McIntosh, R.; Rosair, G. M.; Welch, A. J. *Chem. Commun.* **2005**, 1917−1919. (e) Evans, W. J.; Hawthorne, M. F. *J. Chem. Soc., Chem. Commun.* **1974**, 38−39.

Table 2. Selected Bond Distances (Å) for **13**, **13a**, **14**, **15**, **15a**, and **17**−**19**

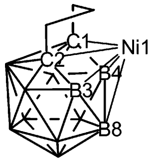

	13[a]	13a	14	15	15a	17	18	19
C(1)−C(2)	1.503(10) [1.552(9)]	1.529(8)	1.552(6)	1.553(5)	1.547(6)	1.541(5)	1.491(6)	1.512(9)
C(1)−B(4)	1.578(11) [1.557(11)]	1.557(6)	1.572(7)	1.562(7)	1.570(8)	1.565(5)	1.739(6)	1.738(11)
C(2)−B(3)	1.573(12) [1.596(12)]	1.557(6)	1.580 (7)	1.560(6)	1.561(8)	1.572(6)	1.730(6)	1.714(11)
B(4)−B(8)	1.874(12) [1.844(11)]	1.903(6)	1.859(7)	1.864(7)	1.860(8)	1.862(5)	1.914(7)	1.947(12)
B(3)−B(8)	1.850(12) [1.894(11)]	1.903(6)	1.893(7)	1.854(7)	1.866(8)	1.879(6)	1.925(7)	1.946(12)
B(3)···B(4)	2.628(18) [2.657(18)]	2.677(6)	2.653(9)	2.584(8)	2.614(10)	2.650(6)	2.854(7)	2.869(12)
d[b]	0.691 [0.695]	0.679	0.705	0.721	0.682	0.701	0.631	0.620
Ni(1)−C(1)							2.216(4)	2.205(7)
Ni(1)−C(2)							2.158(4)	2.195(7)
Ni(1)−B(3)							2.061(5)	2.051(8)
Ni(1)−B(4)							2.062(5)	2.058(8)
Ni(1)−B(8)							2.469(5)	2.451(8)

[a] Distances in brankets are those of a second molecule. [b] Displacement of B(8) to the C(1)C(2)B(3)B(4) plane.

Scheme 5. Preparation of Group 2 Metal Complexes of 13-Vertex *nido*-Carboranes

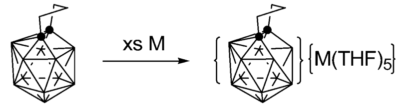

2

M = Mg (**16**), Ca (**17**)

Scheme 6. Preparation of 14-Vertex Nickelacarboranes

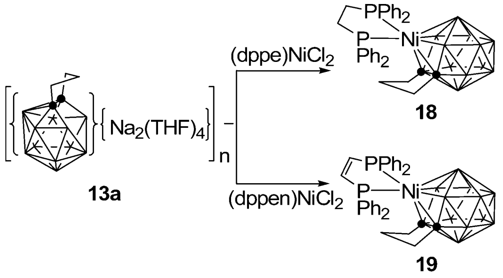

13a

18

19

of the very strong reducing power of 13-vertex *nido*-carborane anions. In the case of $(Ph_3P)_2NiCl_2$ and $(Ph_3P)_3RuCl_2$, the ^{11}B NMR spectra indicated the formation of new products in addition to **2**. Many attempts to isolate a pure 14-vertex species from the reaction mixtures failed.

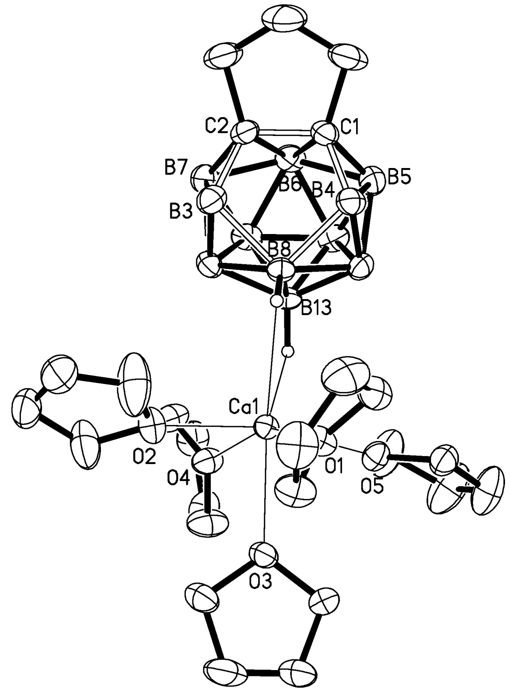

Figure 10. Molecular structure of $\{1,2\text{-}(CH_2)_3\text{-}1,2\text{-}C_2B_{11}H_{11}\}\{Ca(THF)_5\}$ (**17**).

The above results suggested that prevention of the redox reactions is crucial for the preparation of 14-vertex metallacarboranes. After screening a number of metal halides, it was found that $(dppe)NiCl_2$[21] and $(dppen)NiCl_2$[22] (dppe = 1,2-bis(diphenylphosphino)ethane, dppen = *cis*-1,2-bis(diphenylphosphino)ethene) were suitable metal salts. They were treated with 1 equiv of **13a** in THF to afford the desired 14-vertex nickelacarboranes $[\eta^5\text{-}(CH_2)_3C_2B_{11}H_{11}]Ni(dppe)$ (**18**) and $[\eta^5\text{-}(CH_2)_3C_2B_{11}H_{11}]Ni(dppen)$ (**19**) in 34% and 45% yields, respectively (Scheme 6). Complexes **18** and **19** were very sensitive to air and moisture. They decomposed slowly at room temperature in solution to generate **2** and presumably $Ni(dppe)_2$ or $Ni(dppen)_2$ as indicated by ^{11}B and ^{31}P NMR. It was noted that **18** and **19** did not dissolve in common organic solvents such as THF and CH_2Cl_2 once crystallized out, which made NMR characterization infeasible. The ^1H NMR spectra of their hydrolysis products showed a ratio of one dppe or dppen and three THF molecules per cage.

Single-crystal X-ray analyses revealed that **18** and **19** are isomorphous and isostructural with three THFs of solvation, as

---

(21) Booth, G.; Chatt, J. *J. Chem. Soc.* **1965**, 3238−3241.

(22) Bomfim, J. A. S.; de Souza, F. P.; Filgueiras, C. A. L.; de Sousa, A. G.; Gambardella, M. T. P. *Polyhedron* **2003**, *22*, 1567−1573.

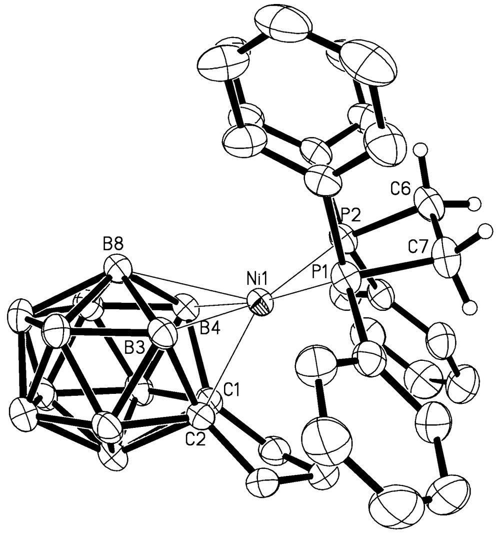

Figure 11. Molecular structure of [η^5-$(CH_2)_3C_2B_{11}H_{11}$]Ni(dppe) (**18**).

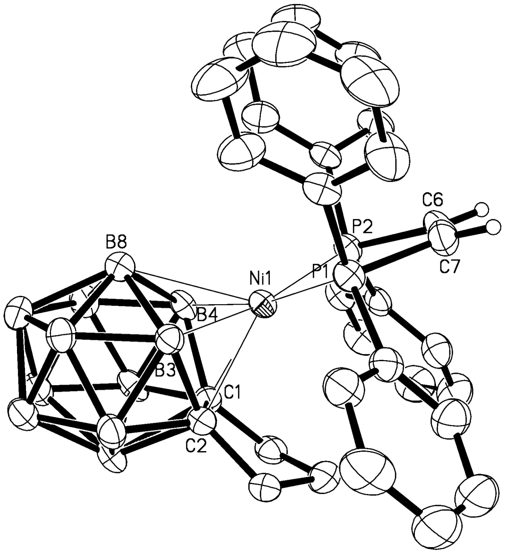

Figure 12. Molecular structure of [η^5-$(CH_2)_3C_2B_{11}H_{11}$]Ni(dppen) (**19**).

shown in Figures 11 and 12, respectively. Selected bond lengths are summarized in Table 2. The geometry of the 14-vertex metallacarborane is a distorted-bicapped-hexagonal antiprism with two seven-coordinate boron vertices, which is similar to the 14-vertex carborane.[7] Different from 13- and 14-vertex metallacarboranes of the C_2B_{10} systems[20a,d] in which the metal is often bound to the carborane cage in an η^6 fashion, the Ni atom in **18** and **19** is bound to the bent open face (C(1)C(2)-B(3)B(4)B(8)) in an η^5 fashion with relatively long Ni(1)−B(8) bond distances of 2.469(5) Å in **18** and 2.451(1) Å in **19**, respectively. The open pentagonal bonding faces in **18** and **19** are much larger than those observed in **13**−**15a** and **17** as indicated by the bond distances (Table 2). On the other hand, the out-of-plane displacement of the B(8) atom is significantly smaller than that found in groups 1 and 2 metal salts of the 13-vertex [*nido*-$(CH_2)_3C_2B_{11}H_{11}$]$^{2-}$. These changes imply that the open bonding face in 13-vertex *nido*-carborane dianion is quite flexible. Except for the Ni(1)−B(8) bond, other Ni−C, Ni−B, and Ni−P bond distances in **18** and **19** (Table 2) are very close to those observed in the known nickelacarboranes such as [η^5-$Ph_2C_2B_9H_9$]Ni(dppe) [23] and [η^5-2,4-$(SiMe_3)_2$-2,4-$C_2B_4H_4$]Ni(TMEDA).[24] Complexes **18** and **19** are best described as 18e$^-$ species, in which *nido*-carboranyl acts as a 6e$^-$ π ligand.

Conclusion

This paper reports in detail the syntheses, properties, and synthetic applications of 13-vertex *closo*- and *nido*-carboranes. The results show that the capitation reactions of CAd 12-vertex *nido*-carborane dianionic salts with dihaloboranes are generally a good method for the preparation of 13-vertex carboranes. The C, C′-linkages of the cages have a large effect on the formation of 13-vertex carboranes. Less sterically demanding linkages and dihaloboranes usually offer higher synthetic yields. These super-carboranes have more diverse structures than their icosahedral cousins. Different isomers are observed in the solid-state structures of 13-vertex species with various connectivity patterns of the cage carbon atoms.

Electrophilic substitution of BH vertices on 13-vertex *closo*-carborane has been achieved. Hexamethylated and hexahalogenated 13-vertex *closo*-carboranes have been prepared. Surprisingly, the latter decomposes slowly upon exposure to moisture, whereas the polyhalogenated icosahedral carboranes are very stable to water.

13-Vertex *closo*-carboranes are readily reduced by groups 1 and 2 metals, affording CAd 13-vertex *nido*-carborane dianions with a bent pentagonal face. These CAd dianions are inert toward Li metal, which is significantly different from their 12-vertex analogues. No CAd 13-vertex *arachno*-carborane tetraanions are observed.

Although CAd 13-vertex carborane dianions are stronger reducing reagents than the corresponding 12-vertex ones as evidenced by the reaction with Li metal, they are new π ligands for transition metals. The isolation and structural characterization of the 14-vertex carborane and nickelacarboranes clearly show that CAd 13-vertex *nido*-carborane dianions are useful synthons for the production of super-carboranes and -heteroboranes. It is anticipated that a new class of 14-vertex heterocarboranes derived from 13-vertex carboranes would be prepared in the foreseeable future.

Experimental Section

General Procedures. All experiments were performed under an atmosphere of dry dinitrogen with the rigid exclusion of air and moisture using standard Schlenk or cannula techniques or in a glovebox. All organic solvents were freshly distilled from sodium benzophenone ketyl immediately prior to use. 1,2-$(CH_2)_3$-1,2-$C_2B_{10}H_{10}$ (**1**),[7] [{1,2-$(CH_2)_3$-1,2-$C_2B_{10}H_{10}$}{$Li_4(THF)_5$}]$_2$ (**6**),[7] [{1,2-$C_6H_4(CH_2)_2$-1,2-$C_2B_{10}H_{10}$}{Li_4-$(THF)_6$}]$_2$ (**7**),[8a] *Z*-EtCH=CEtBBr$_2$·SMe$_2$,[25] *E*-^{t}BuCH=CHBBr$_2$·SMe$_2$,[25] activated Mg and Ca powder,[26] (dppe)NiCl$_2$,[21] and (dppen)NiCl$_2$[22] were prepared according to the literature methods. All other chemicals were purchased from either Aldrich or Acros Chemical Co. and used as received unless otherwise noted. Infrared spectra were obtained from KBr pellets prepared in the glovebox on a Perkin-Elmer 1600 Fourier transform spectrometer. ^1H and ^{13}C NMR spectra were recorded on a Bruker DPX 300 spectrometer at 300.13 and 75.47 MHz, respectively. ^{11}B NMR spectra were recorded on a Varian Inova 400 spectrometer at 128.32 MHz. All chemical shifts were reported in δ units with

---

(23) Garrioch, R. M.; Kuballa, P.; Low, K. S.; Rosair, G. M.; Welch, A. J. *J. Organomet. Chem.* **1999**, *575*, 57−62.

(24) Zhang, H.; Wang, Y.; Saxena, A. K.; Oki, A. R.; Maguire, J. A.; Hosmane, N. S. *Organometallics* **1993**, *12*, 3933−3944.

(25) Brown, H. C.; Campbell, J. B., Jr. *J. Org. Chem.* **1980**, *45*, 389−395.

(26) Rieke, R. D.; Li, P. T.-J.; Burns, T. P.; Uhm, S. T. *J. Org. Chem.* **1981**, *46*, 4323−4324.

references to the residual protons of the deuterated solvents for proton and carbon chemical shifts and to external $BF_3\cdot OEt_2$ (0.00 ppm) for boron chemical shifts. Mass spectra were recorded on a Thermo Finnigan MAT 95 XL spectrometer. Elemental analyses were performed by MEDAC Ltd., Middlesex, U.K.

Preparation of $1,2\text{-}(CH_2)_3\text{-}1,2\text{-}C_2B_{11}H_{11}$ (2). To a THF (30 mL) solution of $1,2\text{-}(CH_2)_3\text{-}1,2\text{-}C_2B_{10}H_{10}$ (**1**; 1.84 g, 10.0 mmol) was added finely cut Na metal (0.50 g, 21.7 mmol) and a catalytic amount of naphthalene (0.10 g, 0.78 mmol), and the mixture was stirred at room temperature for 4 days, giving a deep green solution. Removal of THF afforded a brown solid, presumably [*nido*-$(CH_2)_3C_2B_{10}H_{10}$][$Na_2(THF)_x$]. Toluene (30 mL) was then added, giving a yellow suspension. $HBBr_2\cdot SMe_2$ (20.0 mL of 1.0 M in dichloromethane, 20.0 mmol) was slowly added to the suspension at −78 °C, and the mixture was stirred at this temperature for 1 h and then at room temperature for 6 h. Chromatographic separation (SiO_2, 300−400 mesh, *n*-hexane as elute) afforded **1** (0.06 g, 3%) and **2** (0.73 g, 37%) both as a white solid. Mp 60−61 °C. ^1H NMR ($CDCl_3$): δ 3.26 (t, $J = 7.5$ Hz, 4H, $CH_2CH_2CH_2$), 2.18 (m, 2H, $CH_2CH_2CH_2$). $^{13}C\{^1H\}$ NMR ($CDCl_3$): δ 49.11 ($CH_2CH_2CH_2$), 25.55 ($CH_2CH_2CH_2$); the cage carbons were not observed. ^{11}B NMR ($CDCl_3$): δ 3.52 (d, $J_{BH} = 186$ Hz, 1B, BH), 0.96 (d, $J_{BH} = 186$ Hz, 5B, BH), −1.19 (d, $J_{BH} = 186$ Hz, 5B, BH). IR (KBr, cm^{-1}): ν_{BH} 2570 (vs). HRMS *m/z* calcd for $C_5H_{17}B_{11}^+$: 195.2457. Found: 195.2455.

Preparation of $1,2\text{-}(CH_2)_3\text{-}3\text{-}Ph\text{-}1,2\text{-}C_2B_{11}H_{10}$ (3). Following the procedures described for **2**, $PhBCl_2$ (2.60 mL, 20.0 mmol) was reacted with a suspension of [*nido*-$(CH_2)_3C_2B_{10}H_{10}$][$Na_2(THF)_x$] (10.0 mmol) in toluene (30 mL). Compounds **1** (0.12 g, 6%) and **3** (0.54 g, 20%) were obtained as a white solid. X-ray-quality crystals of **3** were grown from a saturated *n*-hexane solution at room temperature. Mp 97−98 °C. ^1H NMR ($CDCl_3$): δ 7.42 (d, $J = 6.9$ Hz, 2H, C_6H_5), 7.32 (m, 3H, C_6H_5), 3.05 (t, $J = 7.2$ Hz, 4H, $CH_2CH_2CH_2$), 1.84 (m, 2H, $CH_2CH_2CH_2$). $^{13}C\{^1H\}$ NMR ($CDCl_3$): δ 134.1, 129.6, 128.1 (C_6H_5), 47.56 ($CH_2CH_2CH_2$), 25.57 ($CH_2CH_2CH_2$); the CB and cage carbons were not observed. ^{11}B NMR ($CDCl_3$): δ 3.31 (s, 1B, BPh), 1.18 (d, $J_{BH} = 186$ Hz, 1B, BH), −2.32 (d, $J_{BH} = 146$ Hz, 3B, BH), −3.30 (d, $J_{BH} = 128$ Hz, 2B, BH), −7.06 (d, $J_{BH} = 166$ Hz, 4B, BH). IR (KBr, cm^{-1}): ν_{BH} 2566 (vs). HRMS *m/z* calcd for $C_{11}H_{21}B_{11}^+$: 270.2578. Found: 270.2581.

Preparation of $1,2\text{-}(CH_2)_3\text{-}3\text{-}(Z\text{-}EtCH{=}CEt)\text{-}1,2\text{-}C_2B_{11}H_{10}$ (4). Following the procedures described for **2**, *Z*-$EtCH{=}CEtBBr_2\cdot SMe_2$ (20.0 mmol in 20 mL of CH_2Cl_2) was reacted with a suspension of [*nido*-$(CH_2)_3C_2B_{10}H_{10}$][$Na_2(THF)_x$] (10.0 mmol) in toluene (30 mL). Compound **4** (0.72 g, 26%) was obtained as a colorless oil with the recovery of **1** (0.10 g, 5%). ^1H NMR ($CDCl_3$): δ 5.73 (t, $J = 7.2$ Hz, 1H, $CH{=}C$), 3.15 (m, 4H, $CH_2CH_2CH_2$), 2.04 (m, 6H, CH_2CH_3 + $CH_2CH_2CH_2$), 0.97 (t, $J = 7.5$ Hz, 3H, CH_2CH_3), 0.88 (t, $J = 7.5$ Hz, 3H, CH_2CH_3). $^{13}C\{^1H\}$ NMR ($CDCl_3$): δ 146.4, 139.2 (vinyl carbon), 47.36 ($CH_2CH_2CH_2$), 25.02 ($CH_2CH_2CH_2$), 22.42 (CH_2CH_3), 22.19 (CH_2CH_3), 14.37 (CH_2CH_3), 13.98 (CH_2CH_3), the cage carbons were not observed. ^{11}B NMR ($CDCl_3$): δ 10.24 (s, 1B, BC), 5.70 (d, $J_{BH} = 145$ Hz, 1B, BH), 2.43 (d, $J_{BH} = 151$ Hz, 4B, BH), 0.31 (d, $J_{BH} = 130$ Hz, 2B, BH), −3.18 (d, $J_{BH} = 153$ Hz, 3B, BH). IR (KBr, cm^{-1}): ν_{BH} 2565 (vs). HRMS *m/z* calcd for $C_{11}H_{27}B_{11}^+$: 278.3204. Found: 278.3204.

Preparation of $1,2\text{-}(CH_2)_3\text{-}3\text{-}(E\text{-}{}^tBuCH{=}CH)\text{-}1,2\text{-}C_2B_{11}H_{10}$ (5). Following the procedures described for **2**, *E*-$^tBuCH{=}CHBBr_2\cdot SMe_2$ (20.0 mmol in 20 mL of CH_2Cl_2) was reacted with a suspension of [*nido*-$(CH_2)_3C_2B_{10}H_{10}$][$Na_2(THF)_x$] (10.0 mmol) in toluene (30 mL). Compound **5** (0.83 g, 30%) was obtained as a colorless oil with the recovery of **1** (0.10 g, 5%). ^1H NMR ($CDCl_3$): δ 6.14 (d, $J = 17.7$ Hz, 1H, $^tBuCH{=}CH$), 5.28 (d, $J = 17.7$ Hz, 1H, $^tBuCH{=}CH$), 3.15 (t, $J = 7.5$ Hz, 4H, $CH_2CH_2CH_2$), 2.05 (m, 2H, $CH_2CH_2CH_2$), 0.99 (s, 9H, $C(CH_3)_3$). $^{13}C\{^1H\}$ NMR ($CDCl_3$): δ 137.0, 128.2 (vinyl carbon), 47.32 ($CH_2CH_2CH_2$), 34.90 ($C(CH_3)_3$), 28.86 ($C(CH_3)_3$), 25.76 ($CH_2CH_2CH_2$); the cage carbons were not observed. ^{11}B NMR ($CDCl_3$): δ 7.03 (s, 1B, BC), 3.12 (d, $J_{BH} = 186$ Hz, 1B, BH), 0.54 (m, 6B, BH), −3.90 (d, $J_{BH} = 128$ Hz, 3B, BH). IR (KBr, cm^{-1}): ν_{BH} 2564 (vs). HRMS *m/z* calcd for $C_{11}H_{27}B_{11}^+$: 278.3204. Found: 278.3200.

Preparation of $1,2\text{-}(CH_2)_3\text{-}1,2\text{-}C_2B_{12}H_{12}$ (8). To a toluene (50 mL) suspension of $[\{1,2\text{-}(CH_2)_3\text{-}1,2\text{-}C_2B_{10}H_{10}\}\{Li_4(THF)_5\}]_2$ (**6**; 8.60 g, 15.0 mmol) was slowly added $HBBr_2\cdot SMe_2$ (75.0 mL of 1.0 M in dichloromethane, 75.0 mmol) at −78 °C, and the mixture was stirred at this temperature for 1 h and then at room temperature for 6 h. Removal of the precipitate and solvents gave a brownish sticky solid. Chromatographic separation (SiO_2, 300−400 mesh, *n*-hexane as elute) afforded **1** (0.12 g, 2%), **2** (1.88 g, 32%), and **8** (0.44 g, 7%), respectively, all as a white solid. Mp 88−90 °C. ^1H NMR ($CDCl_3$): δ 3.15 (m, 4H, $CH_2CH_2CH_2$), 2.31 (m, 2H, $CH_2CH_2CH_2$). $^{13}C\{^1H\}$ NMR ($CDCl_3$): δ 40.73 ($CH_2CH_2CH_2$), 25.88 ($CH_2CH_2CH_2$); the cage carbons were not observed. ^{11}B NMR ($CDCl_3$): δ 7.80 (d, $J_{BH} = 154$ Hz, 1B, BH), 5.64 (d, $J_{BH} = 154$ Hz, 2B, BH), 2.87 (d, $J_{BH} = 160$ Hz, 2B, BH), −4.23 (d, $J_{BH} = 180$ Hz, 1B, BH), −6.39 (d, $J_{BH} = 151$ Hz, 2B, BH), −9.29 (d, $J_{BH} = 168$ Hz, 1B, BH), −12.34 (d, $J_{BH} = 159$ Hz, 2B, BH), −24.73 (d, $J_{BH} = 145$ Hz, 1B, BH). IR (KBr, cm^{-1}): ν_{BH} 2566 (vs). HRMS: *m/z* calcd for $C_5H_{18}B_{12}^+$: 208.2592. Found: 208.2583.

Preparation of $1,2\text{-}C_6H_4(CH_2)_2\text{-}1,2\text{-}C_2B_{11}H_{11}$ (9). Following the procedures described for **8**. $HBBr_2\cdot SMe_2$ (25.0 mL of 1.0 M in dichloromethane, 25.0 mmol) was reacted with $[\{1,2\text{-}C_6H_4(CH_2)_2\text{-}1,2\text{-}C_2B_{10}H_{10}\}\{Li_4(THF)_6\}]_2$ (**7**; 7.20 g, 5.0 mmol) in toluene (30 mL). $1,2\text{-}C_6H_4(CH_2)_2\text{-}1,2\text{-}C_2B_{10}H_{10}$ (0.21 g, 8%) and **9** (0.42 g, 17%) were obtained both as a white solid. X-ray-quality crystals of **9** were grown from a saturated *n*-hexane solution at room temperature. Mp 106−108 °C. ^1H NMR ($CDCl_3$): δ 7.53 (m, 2H, C_6H_4), 7.45 (m, 2H, C_6H_4), 4.35 (s, 4H, CH_2). $^{13}C\{^1H\}$ NMR ($CDCl_3$): δ 130.8, 128.5, 126.6 (C_6H_4), 50.81 (CH_2); the cage carbons were not observed. ^{11}B NMR ($CDCl_3$): δ 4.98 (d, $J_{BH} = 128$ Hz, 1B, BH), 2.11 (d, $J_{BH} = 128$ Hz, 5B, BH), −0.10 (d, $J_{BH} = 146$ Hz, 5B, BH). IR (KBr, cm^{-1}): ν_{BH} 2566 (vs). HRMS *m/z* calcd for $C_{10}H_{19}B_{11}^+$: 256.2421. Found: 256.2424.

Preparation of $8,9,10,11,12,13\text{-}(CH_3)_6\text{-}1,2\text{-}(CH_2)_3\text{-}1,2\text{-}C_2B_{11}H_5$ (10). To an iodomethane (10 mL) solution of **2** (196 mg, 1.00 mmol) was added a catalytic amount of $AlCl_3$ (33 mg, 0.25 mmol), and the mixture was stirred at room temperature for 2 days to give a red-brown turbid solution. After filtration, the solid was washed with *n*-hexane (10 mL × 2). The combined organic solution was treated with a saturated $NaHCO_3$ solution to remove acid and then with an aqueous $Na_2S_2O_3$ solution. After drying with $MgSO_4$, removal of the solvent yielded a pale yellow oil. Flash chromatographic separation (SiO_2, 300−400 mesh, *n*-hexane as elute) afforded **10** (234 mg, 85%) as a white solid. X-ray-quality crystals were grown from a saturated *n*-hexane solution at room temperature. Mp 125−128 °C. ^1H NMR ($CDCl_3$): δ 3.10 (t, $J = 6.0$ Hz, 4H, $CH_2CH_2CH_2$), 2.06 (m, 2H, $CH_2CH_2CH_2$), 0.17 (br, 15H, CH_3), −0.12 (br, 3H, CH_3). $^{13}C\{^1H\}$ NMR ($CDCl_3$): δ 124.4 (cage carbon), 47.97 ($CH_2CH_2CH_2$), 25.23 ($CH_2CH_2CH_2$), 0.92 (br, CH_3). ^{11}B NMR ($CDCl_3$): δ 7.11 (s, 1B, BMe), 5.19 (s, 5B, BMe), −9.41 (d, $J_{BH} = 146$ Hz, 5B, BH). IR (KBr, cm^{-1}): ν_{BH} 2557 (s). HRMS *m/z* calcd for $C_{11}H_{29}B_{11}^+$: 279.3282. Found: 279.3280.

Preparation of $8,9,10,11,12,13\text{-}Br_6\text{-}1,2\text{-}(CH_2)_3\text{-}1,2\text{-}C_2B_{11}H_5$ (11). To a CH_2Cl_2 (10 mL) solution of **2** (196 mg, 1.00 mmol) was added excess bromine (1.58 g, 10.0 mmol) and a catalytic amount of $AlCl_3$ (33 mg, 0.25 mmol), and the mixture was stirred at room temperature for 12 h to give a deep red turbid solution. After filtration, the solid was washed with CH_2Cl_2 (10 mL × 2). The combined organic solution was treated with a cold saturated $NaHCO_3$ aqueous solution and dried with $MgSO_4$. Removal of the solvent yielded a brown solid. Recrystallization from dry CH_2Cl_2 afforded **11** (168 mg, 25%) as yellow crystals. Mp. 181 °C (dec). ^1H NMR ($CDCl_3$): δ 3.30 (t, $J = 7.5$ Hz, 4H, $CH_2CH_2CH_2$), 2.34 (m, 2H, $CH_2CH_2CH_2$). $^{13}C\{^1H\}$ NMR ($CDCl_3$): δ 122.5 (cage carbon), 48.93 ($CH_2CH_2CH_2$), 25.47 ($CH_2CH_2CH_2$). ^{11}B NMR ($CDCl_3$): δ 7.34 (s, 1B, BBr), 1.14 (s, 5B, BBr), −7.91

(d, J_{BH} = 169 Hz, 5B, *B*H). IR (KBr, cm^{-1}): ν_{BH} 2592 (s). HRMS: *m/z* calcd for $C_5H_{11}B_{11}Br_6^+$: 669.6990. Found: 669.6964.

Preparation of 8,9,10,11,12,13-I_6-1,2-$(CH_2)_3$-1,2-$C_2B_{11}H_5$ (12). To a CH_2Cl_2 (10 mL) solution of **2** (196 mg, 1.00 mmol) was added excess iodine (2.54 g, 10.0 mmol) and a catalytic amount of $AlCl_3$ (33 mg, 0.25 mmol), and the mixture was stirred at room temperature for 3 days to give a deep red turbid solution. After filtration, the solid was washed with CH_2Cl_2 (10 mL × 2). The combined organic solution was treated with saturated $NaHCO_3$ solution and then an aqueous $Na_2S_2O_3$ solution and dried with $MgSO_4$. Removal of the solvent yielded a dark red solid. Recrystallization from dry CH_2Cl_2 afforded **12** (210 mg, 22%) as deep red crystals. Mp 230 °C (dec). ^{1}H NMR ($CDCl_3$): δ 3.01 (t, *J* = 7.2 Hz, 4H, $CH_2CH_2CH_2$), 2.30 (m, 2H, $CH_2CH_2CH_2$). The ^{13}C NMR spectrum was not obtained for the very poor solubility of **12** in $CDCl_3$. ^{11}B NMR ($CDCl_3$): δ 2.90 (s, 1B, *B*I), −1.92 (d, J_{BH} = 176 Hz, 5B, *B*H), −8.73 (s, 5B, *B*I). IR (KBr, cm^{-1}): ν_{BH} 2592 (w). HRMS: *m/z* calcd for $C_5H_{11}B_{11}I_6^+$: 951.6220. Found: 951.6220.

Preparation of {1,2-$(CH_2)_3$-1,2-$C_2B_{11}H_{11}$}{$Li_2(DME)_2(THF)_2$} (13). To a THF (10 mL) solution of 1,2-$(CH_2)_3$-1,2-$C_2B_{11}H_{11}$ (**2**; 196 mg, 1.00 mmol) was added finely cut Li metal (90.0 mg, 10.0 mmol), and the mixture was stirred at room temperature for 1 day to give a red solution. Removal of excess Li and THF yielded a pale yellow solid. Recrystallization from DME afforded **13** as colorless crystals (443 mg, 83%). ^{1}H NMR (pyridine-d_5): δ 3.66 (m, 8H, THF), 3.50 (m, 8H, DME), 3.28 (m, 12H, DME), 2.40 (m, 4H, $CH_2CH_2CH_2$), 2.21 (m, 2H, $CH_2CH_2CH_2$), 1.65 (m, 8H, THF). ^{13}C{^{1}H} NMR (pyridine-d_5): δ 71.44, 58.05 (DME), 67.32, 25.25 (THF), 43.21 ($CH_2CH_2CH_2$), 29.26 ($CH_2CH_2CH_2$); the cage carbons were not observed. ^{11}B{^{1}H} NMR (pyridine-d_5): δ −8.67 (1), −14.36 (5), −24.56 (5). IR (KBr, cm^{-1}): ν_{BH} 2427 (vs). Anal. Calcd for $C_{19}H_{49}B_{11}Li_2O_{10.5}$ (**13** − 0.5 THF): C, 45.79; H, 9.91. Found: C, 45.79; H, 9.96.

Preparation of [{1,2-$(CH_2)_3$-1,2-$C_2B_{11}H_{11}$}{$Na_2(THF)_4$}]$_n$ (13a). This complex was prepared as colorless crystals using the same procedures described for **13** from 1,2-$(CH_2)_3$-1,2-$C_2B_{11}H_{11}$ (**2**; 196 mg, 1.00 mmol) and finely cut Na metal (230 mg, 10.0 mmol) in THF (25 mL): yield 425 mg (80%). ^{1}H NMR (pyridine-d_5): δ 3.63 (m, 16H, THF), 2.46 (t, *J* = 6.3 Hz, 4H, $CH_2CH_2CH_2$), 2.25 (m, 2H, $CH_2CH_2CH_2$), 1.59 (m, 16H, THF). ^{13}C{^{1}H} NMR (pyridine-d_5): δ 67.15, 25.11 (THF), 42.93 ($CH_2CH_2CH_2$), 29.24 ($CH_2CH_2CH_2$), the cage carbons were not observed. ^{11}B{^{1}H} NMR (pyridine-d_5): δ −9.01 (1), −14.67 (5), −24.64 (5). IR (KBr, cm^{-1}): ν_{BH} 2501 (vs). Anal. Calcd for $C_{17}H_{41}B_{11}Na_2O_3$ (**13a** − THF): C, 44.54; H, 9.02. Found: C, 44.20; H, 9.03.

Preparation of [{1,2-$(CH_2)_3$-3-Ph-1,2-$C_2B_{11}H_{10}$}{$Na_2(THF)_4$}]$_n$ (14). This complex was prepared as colorless crystals using the same procedures described for **13** from 1,2-$(CH_2)_3$-3-Ph-1,2-$C_2B_{11}H_{10}$ (**3**; 272 mg, 1.00 mmol) and finely cut Na metal (230 mg, 10.0 mmol) in THF (25 mL): yield 515 mg (85%). ^{1}H NMR (pyridine-d_5): δ 8.40 (d, *J* = 6.9 Hz, 2H, C_6H_5), 7.24 (m, 2H, C_6H_5), 7.13 (m, 1H, C_6H_5), 3.65 (m, 16H, THF), 2.38 (m, 4H, $CH_2CH_2CH_2$), 2.20 (m, 2H, $CH_2CH_2CH_2$), 1.61 (m, 16H, THF). ^{13}C{^{1}H} NMR (pyridine-d_5): δ 134.3, 125.7 (C_6H_5), 67.18, 25.14 (THF), 41.07 ($CH_2CH_2CH_2$), 29.22 ($CH_2CH_2CH_2$); the *C*B and cage carbons were not observed. ^{11}B{^{1}H} NMR (pyridine-d_5): δ −5.51 (1), −8.92 (1), −11.68 (2), −17.61 (3), −22.26 (2), −26.08 (1), −27.22 (1). IR (KBr, cm^{-1}): ν_{BH} 2596 (vs). Anal. Calcd for $C_{19}H_{39}B_{11}Na_2O_2$ (**14** − 2THF): C, 49.14; H, 8.46. Found: C, 49.20; H, 8.43.

Preparation of [{1,2-$C_6H_4(CH_2)_2$-1,2-$C_2B_{11}H_{11}$}{$Na_2(THF)_4$}]$_n$ (15). This complex was prepared as colorless crystals using the same procedures described for **13** from 1,2-$C_6H_4(CH_2)_2$-1,2-$C_2B_{11}H_{11}$ (**9**; 258 mg, 1.00 mmol) and finely cut Na metal (230 mg, 10.0 mmol) in THF (25 mL): yield 504 mg (85%). ^{1}H NMR (pyridine-d_5): δ 7.26 (m, 2H, C_6H_4), 7.14 (m, 2H, C_6H_4), 3.65 (m, 16H, THF), 3.37 (s, 4H, CH_2), 1.60 (m, 16H, THF). ^{13}C{^{1}H} NMR (pyridine-d_5): δ 142.6, 126.1, 124.7 (C_6H_4), 67.18, 25.14 (THF), 46.55 (CH_2); the cage carbons were not observed. ^{11}B{^{1}H} NMR (pyridine-d_5): −6.77 (1), −12.55 (5), −23.38 (5). IR (KBr, cm^{-1}): ν_{BH} 2524 (vs). Anal. Calcd for $C_{22}H_{43}B_{11}Na_2O_3$ (**15** − THF): C, 50.77; H, 8.33. Found: C, 51.11; H, 8.48.

Preparation of [{1,2-$C_6H_4(CH_2)_2$-1,2-$C_2B_{11}H_{11}$}{$Na_2(dioxane)_{0.5}(THF)_4$}]$_n$ (15a). This compound was prepared from the recrystallization of **15** (593 mg, 1.00 mmol) in dioxane: yield 540 mg (85%). ^{1}H NMR (pyridine-d_5): δ 7.26 (m, 2H, C_6H_4), 7.14 (m, 2H, C_6H_4), 3.65 (m, 16H, THF), 3.62 (m, 4H, dioxane), 3.37 (s, 4H, CH_2), 1.60 (m, 16H, THF). ^{13}C{^{1}H} NMR (pyridine-d_5): δ 142.6, 126.1, 124.7 (C_6H_4), 67.18, 25.14 (THF), 66.51 (dioxane), 46.55 (CH_2); the cage carbons were not observed. ^{11}B{^{1}H} NMR (pyridine-d_5): δ −6.77 (1), −12.55 (5), −23.38 (5). IR (KBr, cm^{-1}): ν_{BH} 2515 (vs). Anal. Calcd for $C_{24}H_{45}B_{11}Na_2O_4$ (**15a** − THF): C, 51.25; H, 8.06. Found: C, 51.33; H, 8.55.

Preparation of {1,2-$(CH_2)_3$-1,2-$C_2B_{11}H_{11}$}{$Mg(THF)_5$} (16). This complex was prepared as a white powder using the same procedures described for **13** from 1,2-$(CH_2)_3$-1,2-$C_2B_{11}H_{11}$ (**2**; 196 mg, 1.00 mmol) and freshly prepared Mg powder (48 mg, 2.00 mmol) in THF (25 mL): yield 448 mg (77%). ^{1}H NMR (pyridine-d_5): δ 3.65 (m, 20H, THF), 2.43 (m, 4H, $CH_2CH_2CH_2$), 2.26 (m, 2H, $CH_2CH_2CH_2$), 1.62 (m, 20H, THF). ^{13}C{^{1}H} NMR (pyridine-d_5): δ 67.18, 25.14 (THF), 42.69 ($CH_2CH_2CH_2$), 29.33 ($CH_2CH_2CH_2$); the cage carbons were not observed. ^{11}B{^{1}H} NMR (pyridine-d_5): δ −9.00 (1), −14.62 (5), −24.62 (5). IR (KBr, cm^{-1}): ν_{BH} 2488 (vs), 2448 (vs), 2348 (s). Anal. Calcd for $C_7H_{21}B_{11}MgO_{0.5}$ (**16** − 4.5 THF): C, 32.78; H, 8.25. Found: C, 32.69; H, 8.62.

Preparation of {1,2-$(CH_2)_3$-1,2-$C_2B_{11}H_{11}$}{$Ca(THF)_5$} (17). This complex was prepared as colorless crystals using the same procedures described for **13** from 1,2-$(CH_2)_3$-1,2-$C_2B_{11}H_{11}$ (**2**; 196 mg, 1.00 mmol) and freshly prepared Ca powder (80 mg, 2.00 mmol) in THF (25 mL): yield 436 mg (73%). ^{1}H NMR (pyridine-d_5): δ 3.65 (m, 20H, THF), 2.47 (m, 6H, CH_2), 1.61 (m, 20H, THF). ^{13}C{^{1}H} NMR (pyridine-d_5): δ 67.15, 25.12 (THF), 42.75 ($CH_2CH_2CH_2$), 29.34 ($CH_2CH_2CH_2$); the cage carbons were not observed. ^{11}B{^{1}H} NMR (pyridine-d_5): δ −11.00 (1), −15.86 (5), −26.10 (5). IR (KBr, cm^{-1}): ν_{BH} 2499 (vs), 2464 (vs). Anal. Calcd for $C_{21}H_{49}B_{11}CaO_4$ (**17** − THF): C, 48.08; H, 9.41. Found: C, 47.69; H, 9.03.

Preparation of [η^5-$(CH_2)_3C_2B_{11}H_{11}$]Ni(dppe) (18). To a THF (10 mL) suspension of (dppe)$NiCl_2$ (528 mg, 1.00 mmol) was slowly added a THF (10 mL) solution of **13a** (563 mg, 1.00 mmol) at −78 °C, and the mixture was then stirred at room temperature for 6 h to give a deep red solution. After filtration, the resulting red solution was concentrated to about 10 mL. Complex **18**·3THF was obtained as dark red crystals after this solution stood at room temperature for 1 day (296 mg, 34%). NMR data were not obtainable as this complex did not redissolve in common organic solvents. IR (KBr, cm^{-1}): ν_{BH} 2529 (vs). Anal. Calcd for $C_{35}H_{49}B_{11}NiOP_2$ (**18** + THF): C, 57.96; H, 6.81. Found: C, 58.22; H, 7.12.

Preparation of [η^5-$(CH_2)_3C_2B_{11}H_{11}$]Ni(dppen) (19). To a THF (10 mL) suspension of (dppen)$NiCl_2$ (526 mg, 1.00 mmol) was slowly added a THF (10 mL) solution of **13a** (563 mg, 1.00 mmol) at −78 °C, and the mixture was then stirred at room temperature for 6 h to give a deep red solution. After filtration, the resulting red solution was concentrated to about 10 mL. Complex **19**·3THF was obtained as dark red crystals after this solution stood at room temperature for 1 day (390 mg, 45%). NMR data were not obtainable as this complex did not redissolve in common organic solvents. IR (KBr, cm^{-1}): ν_{BH} 2532 (vs). Anal. Calcd for $C_{31}H_{39}B_{11}NiP_2$ (**19**): C, 57.18; H, 6.04. Found: C, 57.52; H, 6.39.

X-ray Structure Determination. Except for **3**, **9**, and **10**, all single crystals were immersed in Paraton-N oil and sealed under N_2 in thin-walled glass capillaries. Data were collected at 293 K on a Bruker SMART 1000 CCD diffractometer using Mo Kα radiation. An empirical absorption correction was applied using the SADABS program.[27] All structures were solved by direct methods and subsequent Fourier difference techniques and refined anisotropically for all non-hydrogen atoms by full-matrix least squares calculations on F^2 using

Table 3. Crystal Data and Summary of Data Collection and Refinement for **3**, **9**, **10**, **11**, and **13**

	3	**9**	**10**	**11**	**13**
formula	$C_{11}H_{21}B_{11}$	$C_{10}H_{19}B_{11}$	$C_{11}H_{29}B_{11}$	$C_5H_{11}B_{11}Br_6$	$C_{42}H_{106}B_{22}Li_4O_{12}$
crystal size (mm^3)	0.40 × 0.30 × 0.10	0.50 × 0.40 × 0.20	0.50 × 0.40 × 0.30	0.30 × 0.20 × 0.10	0.20 × 0.20 × 0.15
fw	272.2	258.2	280.3	669.5	1068.9
crystal system	orthorhombic	orthorhombic	orthorhombic	orthorhombic	orthorhombic
space group	$Pca2_1$	$Pca2_1$	$Pnma$	$Pbca$	$Pca2_1$
a, Å	17.164(1)	29.984(2)	13.549(12)	12.435(2)	26.847(2)
b, Å	12.497(1)	6.958(1)	10.789(9)	17.434(3)	11.269(1)
c, Å	30.441(2)	14.805(1)	12.519(11)	17.516(3)	22.190(2)
V, Å^3	6529.3(7)	3088.5(3)	1830(3)	3797.3(10)	6713.4(9)
Z	16	8	4	8	4
D_{calcd}, Mg/m^3	1.108	1.110	1.017	2.398	1.058
radiation (λ), Å	Mo Kα (0.710 73)	Mo Kα (0.710 73)	Mo Kα (0.710 73)	Mo Kα (0.710 73)	Mo Kα (0.710 73)
2θ range, deg	2.6 to 52.0	2.7 to 56.0	5.0 to 48.0	4.6 to 50.0	3.4 to 48.0
μ, mm^{-1}	0.052	0.052	0.047	12.670	0.065
F(000)	2272	1072	600	2448	2304
no. of obsd reflns	10 488	7358	1523	3344	10 527
no. of params refnd	795	380	136	199	722
goodness of fit	0.960	0.994	1.610	1.017	0.994
R1	0.066	0.060	0.092	0.062	0.090
wR2	0.155	0.135	0.311	0.156	0.222

Table 4. Crystal Data and Summary of Data Collection and Refinement for **14**, **15**, **15a**, **17**, **18**·3THF, and **19**·3THF

	14	**15**	**15a**	**17**	**18**·3THF	**19**·3THF
formula	$C_{27}H_{53}B_{11}Na_2O_4$	$C_{52}H_{102}B_{22}Na_4O_8$	$C_{28}H_{53}B_{11}Na_2O_5$	$C_{25}H_{57}B_{11}CaO_5$	$C_{43}H_{65}B_{11}NiO_3P_2$	$C_{43}H_{63}B_{11}NiO_3P_2$
crystal size (mm^3)	0.50 × 0.40 × 0.30	0.30 × 0.20 × 0.10	0.50 × 0.30 × 0.20	0.25 × 0.20 × 0.15	0.30 × 0.30 × 0.20	0.30 × 0.20 × 0.10
fw	606.6	1185.1	634.6	596.7	869.5	867.5
crystal system	monoclinic	orthorhombic	monoclinic	monoclinic	triclinic	triclinic
space group	$P2_1/n$	$Pbca$	$P2_1/n$	$P2_1/c$	$P\bar{1}$	$P\bar{1}$
a, Å	15.322(5)	11.734(1)	10.662(1)	9.824(1)	11.002(1)	10.961(2)
b, Å	11.640(4)	24.069(1)	28.285(2)	19.279(2)	11.663(1)	11.703(2)
c, Å	20.559(7)	24.633(1)	12.822(1)	18.281(2)	20.388(2)	20.509(3)
α, deg	90	90	90	90	81.85(1)	82.87(1)
β, deg	96.73(1)	90	100.73(1)	92.97(1)	77.99(1)	80.04(1)
γ, deg	90	90	90	90	68.84(1)	67.55(1)
V, Å^3	3641(2)	6956.7(6)	3799.1(5)	3457.9(5)	2380.1(4)	2389.9(7)
Z	4	8	4	4	2	2
D_{calcd}, Mg/m^3	1.106	1.132	1.109	1.146	1.213	1.205
radiation (λ), Å	Mo Kα (0.710 73)	Mo Kα (0.710 73)	Mo Kα (0.710 73)	Mo Kα (0.710 73)	Mo Kα (0.710 73)	Mo Kα (0.710 73)
2θ range, deg	3.2 to 50.0	3.4 to 50.0	2.9 to 48.0	4.2 to 50.0	3.8 to 50.0	2.0 to 48.0
μ, mm^{-1}	0.085	0.088	0.087	0.214	0.512	0.510
F(000)	1296	2528	1352	1288	920	916
no. of obsd reflns	6394	6117	5966	6090	8281	7514
no. of params refnd	397	432	459	380	541	541
goodness of fit	1.014	1.062	1.040	1.023	1.012	1.019
R1	0.088	0.080	0.098	0.058	0.064	0.079
wR2	0.245	0.221	0.274	0.150	0.175	0.203

the SHELXTL program package.[28] All hydrogen atoms were geometrically fixed using the riding model. There were four crystallographically independent molecules in the unit cell of **3** and two in **9** and **13**, respectively. The molecular structures of **18** and **19** contained three THFs of solvation. Crystal data and details of data collection and structure refinements were given in Tables 3 and 4.

Acknowledgment. The work described in this paper was supported by a grant from the Research Grants Council of the Hong Kong Special Administration Region (Project No. 403805).

Supporting Information Available: Crystallographic data in CIF format for complexes **3**, **9**, **10**, **11**, **13**, **14**, **15**, **15a**, and **17**−**19**. This material is available free of charge via the Internet at http://pubs.acs.org.

JA0605772

---

(27) Sheldrick, G. M. *SADABS: Program for Empirical Absorption Correction of Area Detector Data*. University of Göttingen: Germany, 1996.
(28) Sheldrick, G. M. *SHELXTL 5.10 for Windows NT: Structure Determination Software Programs*. Bruker Analytical X-ray Systems, Inc.: Madison, Wisconsin, USA, 1997.